

Article

Physiological and Proteomic Responses of Pitaya to PEG-Induced Drought Stress

Aihua Wang^{1,2}, Chao Ma², Hongye Ma², Zhilang Qiu¹  and Xiaopeng Wen^{1,*} 

- ¹ Key Laboratory of Plant Resource Conservation and Germplasm Innovation in Mountainous Region (Ministry of Education), Collaborative Innovation Center for Mountain Ecology & Agro-Bioengineering (CICMEAB), Institute of Agro-Bioengineering, College of Life Sciences, Guizhou University, Guiyang 550025, China; 118wah@163.com (A.W.); 18786621377@163.com (Z.Q.)
- ² Institute of Horticulture, Guizhou Academy of Agricultural Sciences, Guiyang 550006, China; machao621@126.com (C.M.); lyhmyyqh@163.com (H.M.)
- * Correspondence: wenxp@gzu.edu.cn

Abstract: Pitaya (*Hylocereus polyrhizus* L.) is highly tolerant to drought stress. Elucidating the response mechanism of pitaya to drought will substantially contribute to improving crop drought tolerance. In the present study, the physiological and proteomic responses of the pitaya cultivar ‘Zihonglong’ were compared between control seedlings and seedlings exposed to drought stress (−4.9 MPa) induced by polyethylene glycol for 7 days. Drought stress obviously enhanced osmolyte accumulation, lipid peroxidation, and antioxidant enzyme activities. Proteomic data revealed drought stress activated several pathways in pitaya, including carbohydrate and energy metabolism at two drought stress treatment time-points (6 h and 3 days). Other metabolic pathways, including those related to aspartate, glutamate, glutathione, and secondary metabolites, were induced more at 3 days than at 6 h, whereas photosynthesis and arginine metabolism were induced exclusively at 6 h. Overall, protein expression changes were consistent with the physiological responses, although there were some differences in the timing. The increases in soluble sugar contents mainly resulted from the degradation and transformation of insoluble carbohydrates. Differentially accumulated proteins in amino acid metabolism may be important for the conversion and accumulation of amino acids. GSH and AsA metabolism and secondary metabolism may play important roles in pitaya as enzymatic and nonenzymatic antioxidant systems. The enhanced carbohydrate and energy metabolism may provide the energy necessary for initiating the above metabolic pathways. The current study provided the first proteome profile of this species exposed to drought stress, and may clarify the mechanisms underlying the considerable tolerance of pitaya to drought stress.

Keywords: pitaya; proteomics; glutathione; drought stress; antioxidant enzymes



Citation: Wang, A.; Ma, C.; Ma, H.; Qiu, Z.; Wen, X. Physiological and Proteomic Responses of Pitaya to PEG-Induced Drought Stress. *Agriculture* **2021**, *11*, 632. <https://doi.org/10.3390/agriculture11070632>

Academic Editor: Pirjo Mäkelä

Received: 10 June 2021

Accepted: 5 July 2021

Published: 6 July 2021

Publisher’s Note: MDPI stays neutral with regard to jurisdictional claims in published maps and institutional affiliations.



Copyright: © 2021 by the authors. Licensee MDPI, Basel, Switzerland. This article is an open access article distributed under the terms and conditions of the Creative Commons Attribution (CC BY) license (<https://creativecommons.org/licenses/by/4.0/>).

1. Introduction

Drought, which can be defined as the absence of adequate moisture for normal plant growth, is increasingly becoming a serious global environmental problem [1]. Arid and semiarid regions make up approximately a third of the total land area worldwide. Global warming, deforestation, and urbanization will likely increase the frequency and severity of drought conditions in many regions [2]. Drought severely limits the geographical distribution and productivity of crops, resulting in substantial yield losses [3]. Therefore, there is a growing demand for new crop varieties with enhanced drought tolerance.

Plants have developed complex mechanisms for sensing water availability and reprogramming their metabolism and growth in response to drought stress, which leads to various morphological, physiological, and molecular changes [4]. The morphological changes mainly include decreased shoot growth, stomatal closure, increased rooting depth, and leaf senescence [5,6]. The primary physiological changes involve the photosynthetic system, osmotic regulatory substances, antioxidant enzymes, and endogenous

hormones [6,7]. Molecular studies have resulted in the identification and cloning of some drought-responsive genes. These genes can be classified into the following two groups: genes encoding functional proteins that directly protect plants against environmental stresses, and genes encoding regulatory proteins (e.g., signaling molecules and transcription factors that control gene expression) [8]. Recently, various techniques such as genomics, transcriptomics, and proteomics have been used to understand the complicated mechanisms of plant drought tolerance [5]. By genomic and transcriptome techniques, many candidate genes and pathways associated with drought-stress tolerance have been identified [3,8]. Because cellular processes are regulated by post-translational modifications, protein–protein interactions, and enzymatic activities, gene-expression analyses should be complemented by additional approaches [9]. Accordingly, proteomic studies have been performed to elucidate stress-tolerance mechanisms [10–13]. Additionally, parallel reaction monitoring (PRM), which was recently developed for targeted mass spectrometry, has been used to validate the accuracy and reliability of proteomic data [14]. Protein expression profiles of many crops, such as tobacco (*Nicotiana tabacum* L.) [10], soybean [*Glycine max* (L.) Merr.] [11], rice (*Oryza sativa* L.) [12], wheat (*Triticum aestivum* L.) [13], and cassava (*Manihot esculenta* Crantz) [5] have been reported under drought conditions. To further characterize the mechanisms underlying plant drought resistance, researchers are increasingly relying on a combination of physiology and proteomics [15,16]. Physiological and proteomic responses of contrasting alfalfa (*Medicago sativa* L.) varieties to PEG-induced osmotic stress have been studied by Zhang et al. [6]. Phenological, morpho-physiological, and proteomic responses of *Triticum boeoticum* Boiss. to drought stress were recorded by Moosavi et al. [15]. Chen et al. reported that physiology and proteomics analyses provided comprehensive insights into the overall and variety-specific mechanisms underlying drought response in tobacco, and that protein profiles were consistent with the physiological performances [16]. These studies revealed more proteins and metabolic pathways that respond to drought stress, and provided important information for elucidating the mechanism network of plant response to drought at the system biology level. To date, however, proteomics studies on pitaya are rare. Moreover, physiological and proteomic analyses to understand the response mechanism of pitaya to drought stress have not been reported.

Pitaya (*Hylocereus polyrhizus* L.), also known as dragon fruit, is a member of the family Cactaceae [17]. The pitaya cultivation area is expanding rapidly in many tropical and subtropical areas worldwide because it produces a nutritionally valuable fruit with an exotic appearance, striking colors, and health-promoting properties [18]. Moreover, pitaya is a highly drought-tolerant plant [19], making it an excellent species for mining plant drought-tolerance proteins. Previous studies on pitaya plant responses to drought stress mostly involved physiological and biochemical analyses, with some applying transcriptomic and microarray technologies to detect drought-related expressed sequence tags [20]. However, there are no reports regarding proteome-level analyses of pitaya responses to drought conditions. The objective of this study was to decipher the response mechanism of pitaya to drought. The stems of pitaya seedlings regarding their osmolyte accumulation, degree of lipid peroxidation, antioxidant enzyme activities, and protein abundance changes in response to drought stress simulated using polyethylene glycol (PEG) 6000 were analyzed. The results of this study provide insights into the drought-tolerance mechanisms of pitaya.

2. Materials and Methods

2.1. Plant Materials and Growth Conditions

Pitaya cultivar ‘Zihonglong’ was provided by the Key Laboratory of Plant Resources Conservation and Germplasm Innovation in the Mountainous Region (Ministry of Education), Institute of Agro-Bioengineering, Guizhou University, China. To ensure the uniformity of the examined plant material, pitaya stem buds from the same clone were rapidly micropropagated and maintained in a growth chamber under controlled conditions (25 °C; 14 h day/10 h night cycle; 60 ± 5% relative humidity; and 300 μmol m⁻² s⁻¹ light intensity) as previously described [19]. After 4 weeks of growth, rooted seedlings similar

in size (7–8 cm tall) were transferred to a nutrient solution developed by Hoagland and Arnon [21]. The nutrient solution was changed every 3 days during the hydroponic culture period and was aerated using an air pump to provide plants with sufficient O₂.

2.2. Stress Treatments

To simulate drought stress, 6-week-old pitaya seedlings were transferred to a nutrient solution with an osmotic potential of -0.49 MPa. The solution was prepared using 20% PEG 6000. Seedlings not subjected to drought stress (0 MPa) were used as the control plants. At specific post-treatment time-points (0, 6, 12, and 18 h, as well as 1, 3, 5, and 7 days), six stems of each time-point from stressed and the corresponding control pitaya seedlings were collected (three biological replicates), immediately frozen in liquid nitrogen, and stored at -80 °C before analyzing their physiological parameters. Based on physiological responses, 6 h and 3 days were selected as the optimal treatment durations for investigating pitaya proteomic responses to drought stress. Therefore, pitaya seedlings exposed to drought stress for 6 h and 3 days were designated as OS6H and OS3D, respectively, with the corresponding controls designated as NS6H and NS3D, respectively. A total of 12 stems of the control and drought-stressed (NS6H, NS3D, OS6H, and OS3D, each for three biological replicates) pitaya seedlings were collected for a quantitative 4D label-free proteomics analysis. Six stems of the controls and drought-stressed (3 for NS6H and 3 for OS6H) pitaya seedlings were collected for verification of the differentially accumulated proteins (DAPs) via PRM. The drought experiment design for pitaya is shown in Figure S1.

2.3. Physiological Measurements

The soluble sugar content was measured using a commercial assay kit (catalog number KT-1-Y) according to the method of Buysse and Merckx [22]. The soluble protein content was measured using a commercial assay kit (catalog number BCAP-1-W) by a Coomassie Blue dye-binding method with bovine serum albumin as the standard [23]. The free proline content was determined by a commercial assay kit (catalog number PRO-1-Y) according to the acid ninhydrin method [24]. The malondialdehyde (MDA) was measured with thiobarbituric acid reaction according to Castrejón and Yatsimirsky [25] as described in a commercial assay kit (catalog number MDA-1-Y). The superoxide anion (O₂⁻) content was determined by a commercial assay kit (catalog number SA-1-G) following the method of Lin et al. [26]. The hydrogen peroxide (H₂O₂) level was measured using a commercial assay kit (catalog number H2O2-1-Y) according to Sima et al. [27]. The superoxide dismutase (SOD) activity was measured using a commercial assay kit (catalog number SOD-1-W) according to García-Triana et al. [28]. The glutathione reductase (GR) activity was assayed using a commercial assay kit (catalog number GR-1-W) as described by Foster and Hess [29]. The ascorbic peroxidase (APX) activity was assayed using a commercial assay kit (catalog number APX-1-W) using the method of Ullah et al. [30]. All commercial assay kits were purchased from Suzhou Keming Biotechnology Co., Ltd., Suzhou, China. Each index was conducted with three technique replicates and three biological replicates.

2.4. Protein Extraction

Total proteins were extracted from the stems of controls and drought-stressed pitaya seedlings according to a slightly modified version of a method described by Zhao et al. [31]. Samples were ground to a powder in liquid nitrogen. The powder was transferred to lysis buffer supplemented with 1% Triton X-100, 10 mM dithiothreitol, and 1% protease inhibitor cocktail in a 5 mL centrifuge tube and then sonicated three times on ice using a high-intensity ultrasonic processor (Scientz Biotechnology Co., Ningbo, China). After adding an equal volume of Tris-saturated phenol (pH 8.0), the mixture was vortexed for 5 min before centrifugation ($5500 \times g$, 10 min, 4 °C). The phenol phase was transferred to a new centrifuge tube and precipitated with five volumes of methanol saturated with ammonium sulfate, which was followed by overnight incubation at -20 °C. After centrifuging at $5500 \times g$ for 10 min at 4 °C, the supernatant was discarded. The remaining precipitate was

washed once with ice-cold methanol and then three times with ice-cold acetone. Finally, proteins were redissolved in 8 M urea and quantified using a BCA Protein Assay kit (Pierce, Rockford, IL, USA).

2.5. Trypsin Digestion

Before the trypsin digestion, the volume of the protein solutions was adjusted so all samples were at the same concentration. To precipitate the proteins, samples were slowly mixed with 20% trichloroacetic acid (final concentration) using a vortexer and then incubated at 4 °C for 2 h. The precipitate was pelleted by centrifugation (4500× g, 5 min, 4 °C) and washed two or three times with precooled acetone. The pelleted proteins were then resuspended using 200 mM triethylammonium bicarbonate. Trypsin was added at a 1:50 trypsin-to-protein mass ratio for overnight digestion at 37 °C. The resulting peptides were reduced with 5 mM dithiothreitol for 30 min at 56 °C and alkylated with 11 mM iodoacetamide for 15 min at room temperature in darkness.

2.6. LC-MS/MS Analysis

The peptides were dissolved in solvent A (0.1% formic acid and 2% acetonitrile in water) and then loaded onto a homemade reversed-phase analytical column (25 cm long, 100 µm internal diameter). Peptides were separated on a nanoElute UHPLC system (Bruker Daltonics, Inc., Billerica, MA, USA) using solvent B (0.1% formic acid in acetonitrile) and the following gradients: 4–22% over 70 min, 22–30% in 14 min, increased to 80% in 3 min, and then held at 80% for 3 min, all at a constant flow rate of 450 nL/min. The peptides were subjected to capillary electrophoresis followed by an analysis using the timsTOF Pro (Bruker Daltonics, Inc., Billerica, MA, USA) mass spectrometry system. The electrospray voltage was 1.6 kV. Precursors and fragments were analyzed at the TOF detector, with an MS/MS scan range of 100 to 1700 m/z. The timsTOF Pro system was operated in the parallel accumulation serial fragmentation (PASEF) mode. Precursors with charge states 0–5 were selected for fragmentation, and 10 PASEF-MS/MS scans were acquired per cycle. Dynamic exclusion was set to 30 s.

2.7. Database Search

The resulting MS/MS data were processed using the Maxquant search engine (version 1.6.6.0). Tandem mass spectra were used to screen the *H. polyrhizus* transcriptome database (comprising 24,810 sequences), which has not yet been published. Trypsin/P was specified as the cleavage enzyme, with up to two missed cleavages allowed. The mass tolerance for precursor ions was set as 20 ppm in the first search and 20 ppm in the main search. The mass tolerance for fragment ions was set as 20 ppm. Carbamidomethylation of Cys was specified as a fixed modification, whereas acetylation of protein N-terminals and oxidation of Met were specified as variable modifications. The false-discovery rate was adjusted to <1% and the minimum score for peptides was set as >40.

2.8. Data Analysis

Physiological status of samples were investigated and presented with quantified data. Statistical analysis was carried out with DPS 7.05 software (China) and Microsoft Excel 2007. Significant differences were assessed by one-way ANOVA followed by post hoc Duncan's multiple range tests ($p < 0.05$ or $p < 0.01$).

Gene ontology (GO) functional annotations were completed using the UniProt-GOA database (<http://www.ebi.ac.uk/GOA/>, accessed on 2 July 2020), and the unannotated proteins were predicted using the InterProScan software. Proteins were classified into the three main GO categories (biological process, cellular component, and molecular function). The Kyoto Encyclopedia of Genes and Genomes (KEGG) database (<https://www.kegg.jp/>, accessed on 2 July 2020) was used to identify enriched pathways. The protein contents of the stressed plants and the controls were compared. The significance of any difference was assessed using the two-sample two-tailed T-test. The protein ratio was calculated by the

mean of three biological replicates. Each index was measured in triplicate. A p -value < 0.05 and a protein ratio > 1.2 were set as the criteria for upregulation, whereas a p -value < 0.05 and a protein ratio < 0.83 were set as the criteria for downregulation. The DAPs annotated with enriched GO terms or assigned to KEGG pathways were analyzed using the two-tailed Fisher's exact test.

3. Results

3.1. Physiological Responses of Pitaya to Drought Stress

The soluble sugar content of pitaya at 6 and 12 h, as well as 3 and 7 days, after starting the drought stress treatment were 1.17, 1.12, 1.11, and 1.21 times higher than the corresponding control levels, respectively (Figure 1a). Compared with the controls, there were no significant differences in the soluble protein and free proline contents before the 3-day time-point, but there was a significant increase afterward (Figure 1b,c). The soluble protein content of the stressed samples was 4.33 mg/g at the beginning of the treatment period and increased to 9.09 mg/g after 7 days (Figure 1b). The free proline content of the stressed samples was 32.77 μ g/g at the beginning of the treatment period and increased to 65.71 μ g/g after 7 days (Figure 1c).

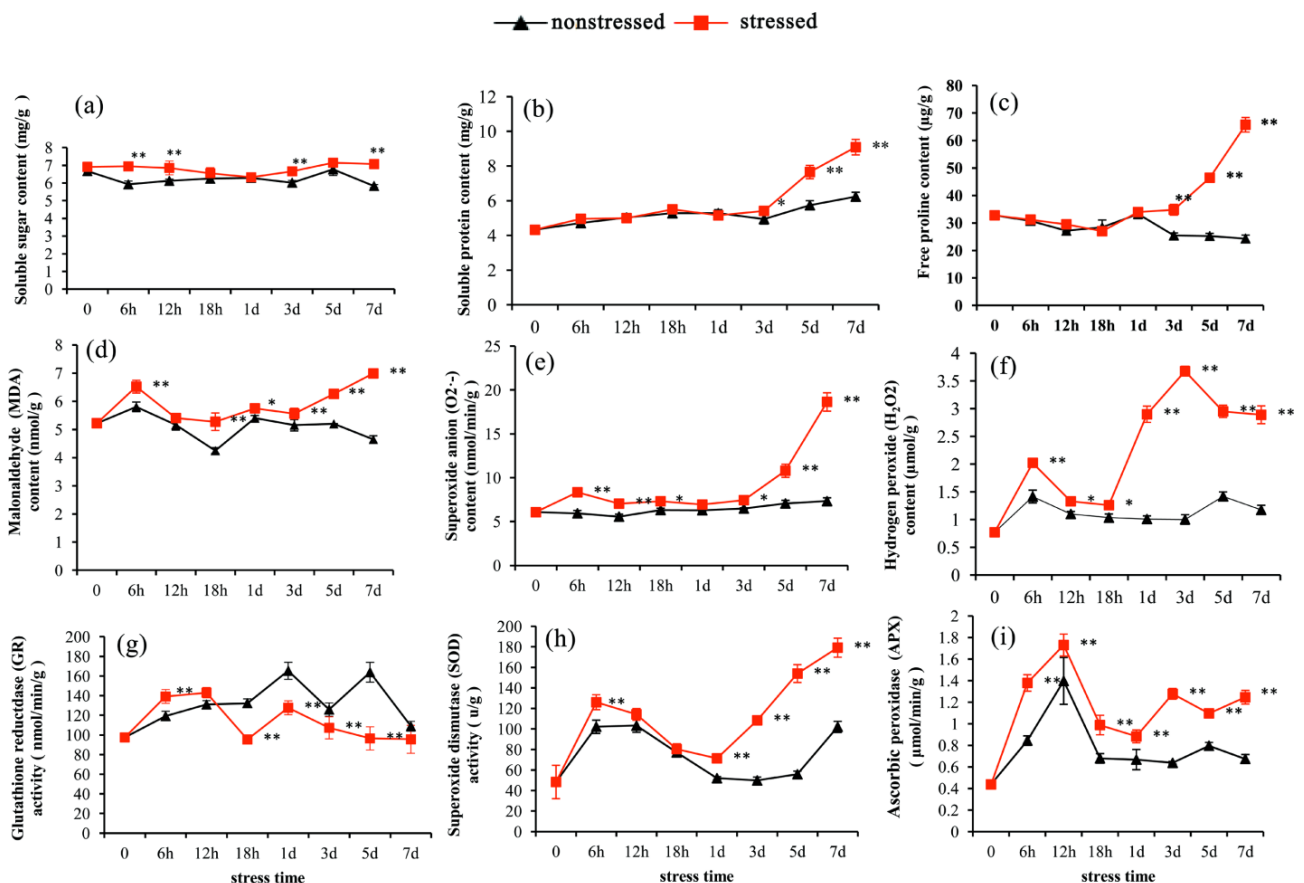


Figure 1. Changes in the soluble sugar (a), soluble protein (b), free proline (c), MDA (d), O_2^- (e), H_2O_2 (f), GR (g), SOD (h), and APX (i) contents in pitaya plants under the control and stressed conditions at different time-points. Asterisks indicate significant differences (* $p < 0.05$, ** $p < 0.01$) from the control. Data are presented as the mean \pm SE of three biological replicates ($n = 3$).

Regarding the lipid peroxidation levels of pitaya, compared with the controls, the MDA and O_2^- contents of the stressed pitaya samples initially increased and then decreased before increasing again during the stress treatment period. Specifically, the MDA and O_2^- contents of the stressed pitaya samples at 6 h were approximately 1.12 and 1.40 times higher, respectively, than the corresponding contents of the controls ($p < 0.01$). After a

slight decrease, the MDA and O₂⁻ contents began to increase again after 3 days of the drought-stress treatment (Figure 1d,e). The H₂O₂ content had a wavelike fluctuating trend as the duration of the drought-stress treatment increased. The H₂O₂ content of stressed pitaya samples first peaked at 6 h (approximately 1.42 times higher than the control level; $p < 0.01$), after which it tended to decrease before increasing to a second peak that was higher than the first one at the 3-day time-point (approximately 3.67 times higher than the control level; $p < 0.01$) and then decreasing again (Figure 1f).

Drought stress significantly affected antioxidant enzyme activities. As the treatment duration increased, the GR activities were significantly higher and lower in the stressed pitaya samples than in the controls at 6 and 18 h, respectively, implying that GR was sensitive to drought stress (Figure 1g). The SOD activities of the stressed pitaya samples first peaked at 6 h (approximately 1.23 times higher than the control level; $p < 0.01$), after which it began to increase again after 1 day (Figure 1h). The APX activities had a wavelike fluctuating trend over the period of the drought-stress treatment. Specifically, the APX activities of the stressed pitaya samples first peaked at 6 h (approximately 1.63 times higher than the control level; $p < 0.01$) and then tended to decrease before increasing to a second peak at 3 days (approximately 2.00 times higher than the control level; $p < 0.01$) (Figure 1i).

3.2. Primary Data Analysis and Protein Detection

To obtain a global overview of the molecular responses of pitaya to drought stress, the proteomes of the stressed and the control stems were compared. Based on the physiological analysis described above, stem samples were collected from stressed and control plants at the 6 h and 3-day time-points for 4D label-free proteomics analysis. A total of 3,107,303 spectra were generated, including 371,016 spectra corresponding to known spectra, 43,489 peptides, 41,084 unique peptides, 5929 identified proteins, and 5269 quantified proteins. The distribution of the number of peptides defining each protein is presented in Figure S2. Most of the proteins included at least two peptides. To clarify the functions of the 5269 quantified proteins, they were annotated according to GO terms, predicted functional domains, KEGG pathways, and KOG functional classifications. Specific details regarding all identified proteins are listed in Table S1.

3.3. Identification and Functional Analysis of DAPs

To identify DAPs, the results of the 4D label-free proteomics analysis were compared as follows: OS6H vs. NS6H and OS3D vs. NS3D. A total of 686 DAPs were identified in these two comparisons. Of these DAPs, 58 (32 upregulated and 26 downregulated) were common to both comparisons, 285 (133 upregulated and 152 downregulated) were specific to the OS6H vs. NS6H comparison, and 343 proteins (154 upregulated and 189 downregulated) were exclusive to the OS3D vs. NS3D comparison (Tables S2 and S3). A Venn diagram was used to illustrate the numbers of significantly upregulated and downregulated proteins in both comparisons (Figure 2). These results reflected the significant differences in the pitaya activities between the stressed and control samples at the two time-points.

The GO annotation and enrichment analysis indicated the identified DAPs were related to 13 biological processes, 9 cellular components, and 10 molecular functions. The number of upregulated proteins annotated with GO terms associated with the prevalent biological processes (e.g., cellular process, metabolic process, response to stimulus, and biological regulation) and the main cellular components (e.g., cell, organelle, membrane, and cell junction) was higher for the OS3D vs. NS3D comparison than for the OS6H vs. NS6H comparison (Figure 3a,b).



Figure 2. Graphical representation and functional cataloging of DAPs. The Venn diagram presents the number of significantly upregulated and downregulated proteins in pitaya under the drought-stress conditions induced by PEG.

The enriched KEGG pathways among the DAPs revealed by the OS6H vs. NS6H and OS3D vs. NS3D comparisons are presented in Figure 4a,b. Among the DAPs in the OS6H vs. NS6H comparison, the four most enriched pathways were carbon metabolism, starch and sucrose metabolism, carbon fixation in photosynthetic organisms, and porphyrin and chlorophyll metabolism (Figure 4a). Of the DAPs in the OS3D vs. NS3D comparison, the three most enriched pathways were starch and sucrose metabolism; pyruvate metabolism; and alanine, aspartate, and glutamate metabolism (Figure 4b). The following eight pathways were enriched among the DAPs in both comparisons: nitrogen metabolism, porphyrin and chlorophyll metabolism, starch and sucrose metabolism, galactose metabolism, arginine and proline metabolism, phenylalanine metabolism, glycolysis/gluconeogenesis, and ascorbate (AsA) and aldarate metabolism. The DAPs related to energy, carbohydrates, amino acids, glutathione (GSH), AsA, and secondary metabolism are examined in greater detail in the following sections.

3.4. DAPs Involved in Carbohydrate Metabolism

Thirty-eight proteins were predicted to be associated with carbohydrate metabolism, with 16 involved in starch and sucrose metabolism, 17 involved in glycolysis, 3 involved in galactose metabolism, and 2 involved in the citrate cycle (TCA cycle) (Table 1). Most of the glycolysis-related enzymes, such as enolase (PGH1), triosephosphate isomerase, phosphoglucomutase (PGMP), glyceraldehyde-3-phosphate dehydrogenase (GAPC), ATP-dependent 6-phosphofructokinase 6 (PFK6), and pyruvate decarboxylase (PDC), were significantly upregulated in pitaya in response to drought stress. Additionally, the accumulation of some key enzymes involved in starch and sucrose metabolism, including isoamylase 3 (ISA3), 4-alpha-glucanotransferase (DPEP), inactive beta-amylase (BAM9), and alpha-amylase 3 (AMY3), increased significantly and promoted starch degradation in pitaya under drought-stress conditions. Interestingly, aldehyde dehydrogenase family 3 members ALDH3F1 and ALDH3H1 exhibited the opposite changes in abundance. A similar difference was detected in the changes to the accumulation of a probable starch synthase 4 (SS4) and starch synthase 1 (SS1).

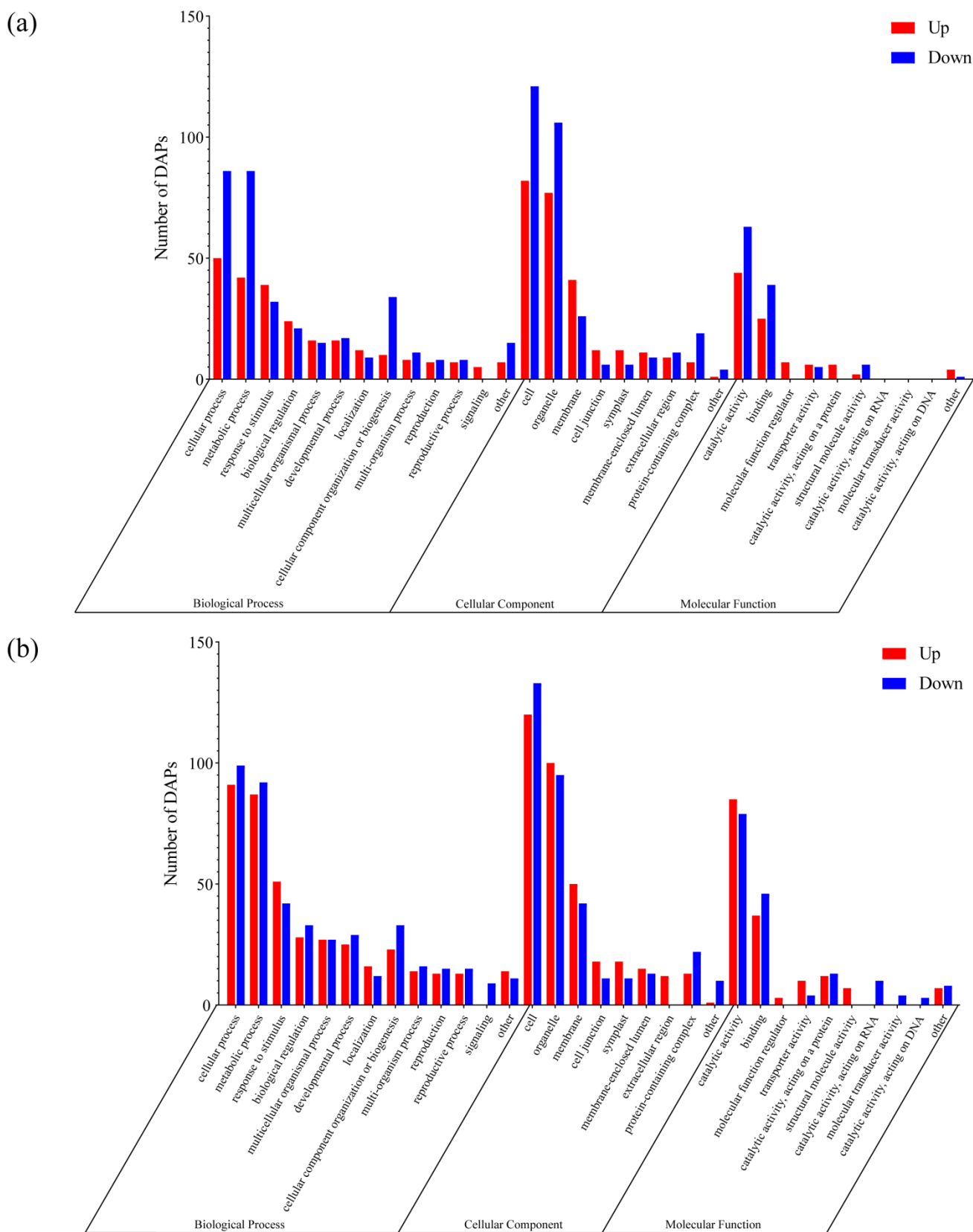


Figure 3. Gene ontology (GO) analysis of DAPs in pitaya stems under drought-stress conditions at 6 h (a) and 3 days (b). Red and blue bars represent upregulated and downregulated proteins, respectively.

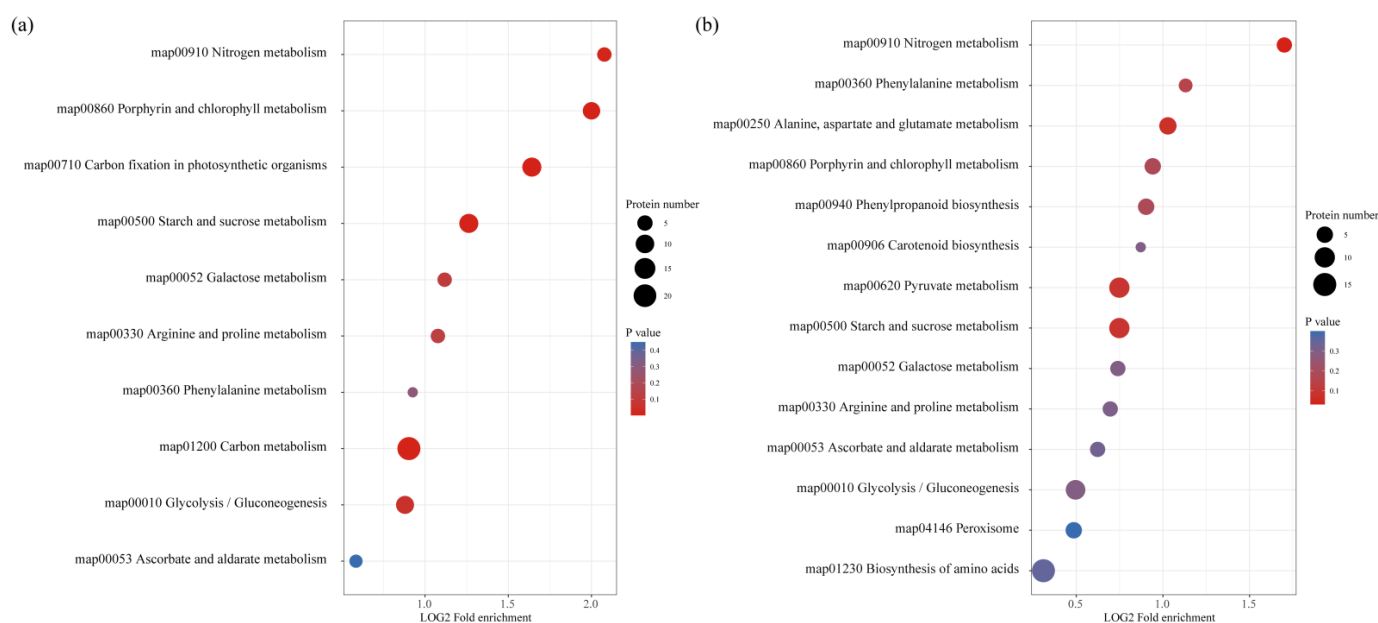


Figure 4. KEGG analysis of DAPs in pitaya stems under drought-stress conditions at 6 h (a) and 3 days (b).

3.5. DAPs Involved in Energy Metabolism

Included among the DAPs were 21 proteins predicted to be associated with energy metabolism, with 10 involved in oxidative phosphorylation, 7 involved in carbon fixation in photosynthetic organisms, and 4 involved in photosynthesis (Table 2). Mitochondrial uncoupling protein 1 (PUMP1) and external alternative NAD(P)H-ubiquinone oxidoreductase B2 (NDB2) associated with oxidative phosphorylation, as well as NADP-dependent malic enzyme-related proteins and phosphoenolpyruvate carboxylase (PPC) associated with carbon fixation in photosynthetic organisms, were upregulated in both comparisons. In contrast, NADH dehydrogenase (ubiquinone) 1 beta subcomplex subunit 9 (CIB22), V-type proton ATPase subunit G1 (VATG1), and acyl carrier protein 2 (MTACP2), associated with oxidative phosphorylation, were upregulated DAPs only in the OS6H vs. NS6H comparison. Additionally, V-type proton ATPase subunit a3 (VHA-a3) and V-type proton ATPase subunit E (VATE), associated with oxidative phosphorylation, were upregulated DAPs only in the OS3D vs. NS3D comparison. Two DAPs, NADH dehydrogenase (ubiquinone) 1 alpha subcomplex subunit 6 (At3g12260) and plasma membrane ATPase 4 (PMA4), associated with oxidative phosphorylation, were downregulated in the OS3D vs. NS3D comparison. The photosynthesis-related DAPs, which were specific to the OS6H vs. NS6H comparison, included an antenna protein (chlorophyll a-b binding protein 7 (LHCB7)) and two photosystem I reaction center subunits (subunit IV (PSAE-1) and subunit VI (PSAH)), which were upregulated, and protease Do-like 2 (DEGP2), which was downregulated. Overall, energy metabolism was enhanced in pitaya under drought-stress conditions.

3.6. DAPs Involved in Amino Acid Metabolism

Of the DAPs induced by drought stress, 14 (5 upregulated and 9 downregulated) were involved in amino acid metabolism (Table 3). Glutamine synthetase (GLN2) was downregulated in both comparisons. Some key enzymes were detected as DAPs only in the OS6H vs. NS6H comparison, including ornithine aminotransferase (δ -OAT), NO-associated protein 1 (NOA1), and spermine synthase (SPMS), which are associated with arginine and proline metabolism. Furthermore, the following proteins were differentially abundant only in the OS3D vs. NS3D comparison: proline-rich receptor-like protein kinase (PERK1), involved in proline metabolism; hydroxyphenylpyruvate reductase (HPPR) and arogenate dehydratase/prephenate dehydratase 6 (ADT6), involved in phenylalanine metabolism; and glutamate decarboxylase (GAD), gamma-aminobutyrate transaminase 3 (GABA-TP3),

aspartate aminotransferase 3 (ASP3), and glutamine synthetase nodule isozyme, involved in aspartate and glutamate metabolism.

3.7. DAPs Involved in GSH and AsA Metabolism

Eleven DAPs were revealed to be involved in GSH and AsA metabolism, including seven involved in AsA metabolism and five involved in GSH metabolism (Table 4). Regarding the AsA metabolism-related proteins, probable 2-oxoglutarate-dependent dioxygenase (At5g05600) and L-ascorbate peroxidase T (APXT) were upregulated DAPs in both comparisons. However, the downregulated proteins UDP-glucose 6-dehydrogenase 4 (UGD4) and UDP-glucose 6-dehydrogenase 5 (UGD5) were detected only in the OS6H vs. NS6H comparison. Additionally, L-galactose dehydrogenase (LGALDH) and L-ascorbate oxidase homolog (Bp10) were detected only in the OS3D vs. NS3D comparison. Moreover, the following four proteins associated with GSH metabolism were upregulated DAPs only in the OS3D vs. NS3D comparison: glutathione S-transferase T1 (GSTT1), IN2-1 homolog B (GSTZ5), and two glucose-6-phosphate 1-dehydrogenase 6 (G6PD6) proteins.

3.8. DAPs Involved in Secondary Metabolism

The DAPs induced by drought stress also contributed to secondary metabolism (Table 5). Specifically, a probable tocopherol O-methyltransferase (VET4), involved in tocopherol synthesis, as well as caffeic acid 3-O-methyltransferase (COMT1), involved in phenylpropanoid synthesis, were upregulated DAPs in both comparisons. Superoxide dismutase (Cu–Zn) (SODCP) in the antioxidation system was an upregulated DAP only in the OS6H vs. NS6H comparison. Seven DAPs were exclusive to the OS3D vs. NS3D comparison, of which peroxidase 4 (GSVIVT00023967001), involved in phenylpropanoid synthesis, as well as a probable carotenoid cleavage dioxygenase 4 (CCD4) and lycopene beta-cyclase (LCY1), involved in carotenoid biosynthesis, were upregulated, whereas omega-hydroxypalmitate O-feruloyl transferase (HHT1) and a probable cinnamyl alcohol dehydrogenase (CAD6), involved in phenylpropanoid synthesis; anthocyanidin-3-O-glucoside rhamnosyltransferase (RT), involved in flavonoid synthesis; and anthocyanidin 3-O-glucosyltransferase 2 (FGT), involved in anthocyanin biosynthesis, were downregulated.

Table 1. DAPs are involved in carbohydrate metabolism.

Protein ID	Description	Protein Abbreviation	OS6H/NS6H Ratio	OS6H/NS6H <i>p</i> -Value	OS3D/NS3D Ratio	OS3D/NS3D <i>p</i> -Value
Glycolysis						
TRINITY_DN1285_c0_g1_m.2918	Pyrophosphate—fructose 6-phosphate 1-phosphotransferase subunit beta	PPF-BETA	1.2232	0.028736	ns	0.491619
TRINITY_DN1345_c0_g1_m.3326	Enolase	PGH1	1.2113	0.023062	ns	0.176205
TRINITY_DN1541_c1_g1_m.4614	Triosephosphate isomerase	–	1.2205	0.048792	ns	0.190237
TRINITY_DN22699_c0_g1_m.8480	Plastidial pyruvate kinase 2	PKP2	0.7949	0.012965	ns	0.071468
TRINITY_DN680_c2_g1_m.20738	Fructose-1,6-bisphosphatase	–	0.6861	0.001059	ns	0.068059
TRINITY_DN700_c0_g1_m.21125	Phosphoglucomutase	PGMP	1.2058	0.003547	ns	0.09038
TRINITY_DN8402_c0_g1_m.23765	Aldehyde dehydrogenase family 3 member F1	ALDH3F1	1.4108	0.034248	1.4821	0.004249
TRINITY_DN956_c0_g1_m.25499	Glyceraldehyde-3-phosphate dehydrogenase	GAPC	1.2105	0.00537	ns	0.23787
TRINITY_DN956_c0_g1_m.25500	Glyceraldehyde-3-phosphate dehydrogenase	GAPC	1.2849	0.006127	ns	0.272781
TRINITY_DN1378_c0_g1_m.3547	ATP-dependent 6-phosphofructokinase 6	PFK6	ns	0.052857	2.8748	0.008707
TRINITY_DN188_c0_g2_m.6607	Aldehyde dehydrogenase family 3 member F1	ALDH3F1	ns	0.102474	0.7175	0.042614
TRINITY_DN2017_c0_g1_m.7240	Pyruvate decarboxylase 4	PDC4	ns	0.091026	1.7692	0.002958
TRINITY_DN2017_c0_g2_m.7243	Pyruvate decarboxylase 1	PDC1	ns	0.087881	1.2044	0.012331
TRINITY_DN2514_c0_g1_m.9503	Aldehyde dehydrogenase family 3 member H1	ALDH3H1	ns	0.724813	0.6052	0.012778
TRINITY_DN5539_c0_g1_m.18129	Alcohol dehydrogenase class-3	–	ns	0.526004	1.2465	0.00285
TRINITY_DN785_c0_g1_m.22777	Hexokinase-3	At1g50460	ns	0.97966423	0.6069	0.002177
Starch and sucrose metabolism						
TRINITY_DN120_c1_g1_m.2258	Beta-fructofuranosidase, soluble isoenzyme I	INV*DC4	1.2139	0.025473	ns	0.36858184
TRINITY_DN1281_c0_g1_m.2874	4-alpha-glucanotransferase	DPEP	1.3783	0.001518	ns	0.065598773
TRINITY_DN2311_c0_g1_m.8701	Alpha-1,4 glucan phosphorylase L isozyme	–	1.2988	0.015376	1.6666	0.033337
TRINITY_DN243_c0_g1_m.9202	Glucose-1-phosphate adenyltransferase large subunit 1	AGPS1	1.3654	0.002383	ns	0.065961158
TRINITY_DN243_c0_g2_m.9203	Glucose-1-phosphate adenyltransferase large subunit 1	AGPS1	1.4417	0.005241	ns	0.082784957
TRINITY_DN3421_c0_g1_m.12709	Probable starch synthase 4	SS4	0.8081	0.000869	ns	0.436338494
TRINITY_DN396_c0_g2_m.14182	Isoamylase 3	ISA3	1.2597	0.038832	2.2276	0.005774
TRINITY_DN558_c0_g2_m.18286	Glucan endo-1,3-beta-glucosidase 1	At1g11820	0.7347	0.009098	ns	0.258131706
TRINITY_DN6728_c0_g1_m.20594	Inactive beta-amylase 9	BAM9	2.8986	5.89E-05	ns	0.422387234
TRINITY_DN8071_c0_g1_m.23172	Glucose-1-phosphate adenyltransferase small subunit	AGPB1	1.3814	0.013501	ns	0.152380603
TRINITY_DN2107_c0_g1_m.7698	Probable alpha,alpha-trehalose-phosphate synthase	TPS11	ns	0.107875285	0.6784	0.047779
TRINITY_DN409_c0_g3_m.14564	Alpha-glucosidase	–	ns	0.145618967	1.3875	0.047325
TRINITY_DN483_c0_g2_m.16576	Alpha-1,4 glucan phosphorylase L isozyme,	–	ns	0.241229313	1.2924	0.04298
TRINITY_DN4852_c0_g1_m.16596	Alpha-amylase 3	AMY3	ns	0.629154053	1.4422	0.043718
TRINITY_DN6640_c0_g1_m.20450	Glucose-1-phosphate adenyltransferase large subunit	AGPS1	ns	0.11514614	1.3167	0.030977
TRINITY_DN7735_c0_g1_m.22545	4-alpha-glucanotransferase	DPEP	ns	0.15889801	1.3818	0.01198
TRINITY_DN8896_c0_g1_m.24535	Starch synthase 1	SS1	ns	0.999352844	1.4676	0.046376

Table 1. Cont.

Protein ID	Description	Protein Abbreviation	OS6H/NS6H Ratio	OS6H/NS6H <i>p</i> -Value	OS3D/NS3D Ratio	OS3D/NS3D <i>p</i> -Value
	Citrate cycle (TCA cycle)					
TRINITY_DN12082_c0_g1_m.2243	Citrate synthase	–	ns	0.664702	1.2021	0.020504
TRINITY_DN3909_c0_g2_m.14018	ATP-citrate synthase alpha chain protein 1	ACLA-1	ns	0.137801	1.2304	0.002227
	Galactose metabolism					
TRINITY_DN455_c0_g1_m.15769	Probable galactinol–sucrose galactosyltransferase 6	RFS6	1.255	0.02696	ns	
TRINITY_DN4902_c0_g1_m.16720	Probable galactinol–sucrose galactosyltransferase 6	RFS6	1.3	0.044023	ns	
TRINITY_DN327_c0_g1_m.12252	Alpha-galactosidase 3	AGAL3	ns		1.4405	0.029031

Note: “–” = not found or did not exist; “ns” = no significant difference. Pitaya seedlings exposed to drought stress for 6 h and 3 days were designated as OS6H and OS3D, respectively, with the corresponding controls designated as NS6H and NS3D, respectively.

Table 2. DAPs are involved in energy metabolism.

Protein ID	Description	Protein Abbreviation	OS6H/NS6H Ratio	OS6H/NS6H <i>p</i> -Value	OS3D/NS3D Ratio	Os3d/NS3d <i>p</i> -Value
	Oxidative phosphorylation					
TRINITY_DN130_c0_g2_m.3091	NADH dehydrogenase (ubiquinone) 1 beta subcomplex subunit 9	CIB22	1.215	0.006	ns	0.481
TRINITY_DN284_c10_g1_m.10791	V-type proton ATPase subunit G 1	VATG1	2.006	0.022	ns	0.355
TRINITY_DN5440_c0_g1_m.17954	External alternative NAD(P)H-ubiquinone oxidoreductase B2	NDB2	1.295	0.024	ns	0.406
TRINITY_DN7109_c0_g2_m.21284	Mitochondrial uncoupling protein 1	PUMP1	1.285	0.006	1.2331	0.016
TRINITY_DN1470_c0_g1_m.4137	V-type proton ATPase subunit a3	VHA-a3	ns	0.059	1.592	0.034
TRINITY_DN30311_c0_g1_m.11465	V-type proton ATPase subunit E	VATE	ns	0.039	1.224	0.025
TRINITY_DN5440_c0_g1_m.17953	External alternative NAD(P)H-ubiquinone oxidoreductase B2	NDB2	ns	0.084	1.202	0.014
TRINITY_DN6767_c0_g2_m.20656	Acyl carrier protein 2	MTACP2	1.264	0.003	ns	0.131
TRINITY_DN10196_c0_g1_m.265	NADH dehydrogenase [ubiquinone] 1 alpha subcomplex subunit 6	At3g12260	ns	0.293	0.826	0.014
TRINITY_DN517_c0_g3_m.17409	Plasma membrane ATPase 4	PMA4	ns	0.15	0.726	0.022
	Carbon fixation in photosynthetic organisms					
TRINITY_DN1003_c0_g1_m.71	NAD-dependent malic enzyme 62 kDa isoform	–	1.2388	0.005	ns	0.196015
TRINITY_DN1003_c0_g1_m.72	NAD-dependent malic enzyme 62 kDa isoform	–	1.2197	0.004638	1.2602	0.018536
TRINITY_DN1199_c0_g1_m.2179	NAD-dependent malic enzyme 59 kDa isoform	–	1.2055	0.012349	ns	0.187842
TRINITY_DN21851_c0_g1_m.8123	NADP-dependent malic enzyme	–	1.4738	0.028002	ns	0.184188

Table 2. Cont.

Protein ID	Description	Protein Abbreviation	OS6H/NS6H Ratio	OS6H/NS6H <i>p</i> -Value	OS3D/NS3D Ratio	Os3d/NS3d <i>p</i> -Value
TRINITY_DN54_c0_g1_m.18065	Phosphoenolpyruvate carboxylase	PPC16	1.3809	0.006254	2.0725	0.015201
TRINITY_DN5722_c0_g1_m.18543	Phosphoenolpyruvate carboxylase 1	PPC1	1.5942	0.029038	2.5273	0.005758
TRINITY_DN5722_c0_g1_m.18545	Phosphoenolpyruvate carboxylase 1 Photosynthesis	PPC1	1.7533	0.024815	1.471	0.019766
TRINITY_DN3928_c2_g1_m.14056	Chlorophyll a-b binding protein 7	LHCB7	1.311	0.048	ns	0.216
TRINITY_DN2207_c0_g1_m.8225	Photosystem I reaction center subunit IV	PSAE-1	1.24	0.003	ns	0.244
TRINITY_DN4734_c0_g1_m.16295	Photosystem I reaction center subunit VI	PSAH	1.422	0.048	ns	0.091
TRINITY_DN2097_c1_g1_m.7621	Protease Do-like 2	DEGP2	0.746	0.007	ns	0.39

Note: “–” = not found or did not exist; “ns” = no significant difference. Pitaya seedlings exposed to drought stress for 6 h and 3 days were designated as OS6H and OS3D, respectively, with the corresponding controls designated as NS6H and NS3D, respectively.

Table 3. DAPs are involved in amino acid metabolism.

Protein ID	Description	Protein Abbreviation	OS6H/NS6H Ratio	OS6H/NS6H <i>p</i> -Value	OS3D/NS3D Ratio	OS3D/NS3D <i>p</i> -Value
	Aspartate and glutamate metabolism					
TRINITY_DN1488_c1_g1_m.4241	Glutamine synthetase	GLN2	0.7957	0.026414	ns	0.97597626
TRINITY_DN1404_c3_g1_m.3689	Glutamate decarboxylase	GAD	ns	0.0013574	1.3966	0.027208
TRINITY_DN294_c0_g1_m.11144	Gamma aminobutyrate transaminase 3	GABA-TP3	ns	0.683342268	1.2024	0.010061
TRINITY_DN7757_c0_g1_m.22593	Aspartate aminotransferase 3	ASP3	ns	0.141381977	1.272	0.00091
TRINITY_DN1488_c1_g1_m.4239	Glutamine synthetase	GLN2	ns	0.064775788	0.8262	0.037899
TRINITY_DN15906_c0_g1_m.4931	Glutamine synthetase nodule isozyme	–	ns	–	0.7607	0.027319
	Arginine and proline metabolism					
TRINITY_DN1617_c1_g1_m.5135	Ornithine aminotransferase	DELTA-OAT	1.2603	0.008374713	ns	0.258228322
TRINITY_DN809_c0_g2_m.23215	Proline-rich receptor-like protein kinase	PERK1	ns	0.160140522	0.7234	0.001426311
TRINITY_DN6277_c0_g2_m.19711	NO-associated protein 1	NOA1	0.8235	0.019199161	ns	0.055348656
TRINITY_DN7062_c0_g1_m.21204	Spermine synthase	SPMS	0.7974	0.014501	ns	0.35623713
	Phenylalanine metabolism					
TRINITY_DN10229_c1_g1_m.315	Hydroxyphenylpyruvate reductase	HPPR	ns	0.735219447	1.2086	0.003324
TRINITY_DN3220_c0_g1_m.12107	Probable enoyl-CoA hydratase 1	ECHIA	0.8204	0.031414137	ns	0.293016083
TRINITY_DN185_c0_g1_m.6424	Histidinol-phosphate aminotransferase	HPA	ns	0.024259888	0.8195	0.015681
TRINITY_DN2397_c0_g1_m.9007	Arogenate dehydratase/prephenate dehydratase 6	ADT6	ns	0.081337319	0.7012	0.012254

Note: “–” = not found or did not exist; “ns” = no significant difference. Pitaya seedlings exposed to drought stress for 6 h and 3 days were designated as OS6H and OS3D, respectively, with the corresponding controls designated as NS6H and NS3D, respectively.

Table 4. DAPs are involved in glutathione and ascorbate metabolism.

Protein ID	Description	Protein Abbreviation	OS6H/NS6H Ratio	OS6H/NS6H <i>p</i> -Value	OS3D/NS3D Ratio	OS3D/NS3D <i>p</i> -Value
	Ascorbate metabolism					
TRINITY_DN1613_c0_g1_m.5115	UDP-glucose 6-dehydrogenase 4	UGD4	0.6064	0.006265	ns	0.151395367
TRINITY_DN1613_c0_g2_m.5117	UDP-glucose 6-dehydrogenase 5	UGD5	0.8276	0.020249	ns	0.671819139
TRINITY_DN1595_c0_g1_m.4962	L-galactose dehydrogenase	LGALDH	ns	0.701474521	1.291	0.036156
TRINITY_DN3248_c0_g1_m.12163	Probable 2-oxoglutarate-dependent dioxygenase	At5g05600	1.8511	0.006704	4.1204	0.0000578
TRINITY_DN893_c0_g1_m.24609	L-ascorbate peroxidase T	APXT	ns	0.841331205	1.2801	0.0015628
TRINITY_DN893_c0_g1_m.24610	L-ascorbate peroxidase T	APXT	1.2609	0.039256535	ns	0.056852039
TRINITY_DN427_c0_g2_m.15091	L-ascorbate oxidase homolog	Bp10	ns	0.562150148	1.2159	0.013967466
	Glutathione metabolism					
TRINITY_DN4975_c0_g1_m.16910	Glutathione S-transferase T1	GSTT1	ns	0.117978	1.6817	0.0466
TRINITY_DN178_c0_g1_m.6079	Protein IN2-1 homolog B	GSTZ5	ns	0.262995961	1.3097	0.011018
TRINITY_DN2046_c0_g1_m.7392	Glucose-6-phosphate 1-dehydrogenase 6	G6PD6	ns	0.019788019	1.2133	0.009388
TRINITY_DN2046_c0_g1_m.7393	Glucose-6-phosphate 1-dehydrogenase 6	G6PD6	ns	0.321337379	1.255	0.04952

Note: “ns” = no significant difference. Pitaya seedlings exposed to drought stress for 6 h and 3 days were designated as OS6H and OS3D, respectively, with the corresponding controls designated as NS6H and NS3D, respectively.

Table 5. DAPs are involved in secondary metabolism.

Protein ID	Description	Protein Abbreviation	OS6H/NS6H Ratio	OS6H/NS6H <i>p</i> -Value	OS3D/NS3D Ratio	OS3D/NS3D <i>p</i> -Value
	Tocopherol					
TRINITY_DN1553_c0_g1_m.4682	Probable tocopherol O-methyltransferase	VET4	1.82	0.014	2.725	0.014
	Flavone and flavonol biosynthesis					
TRINITY_DN12687_c0_g1_m.2773	Anthocyanidin-3-O-glucoside rhamnosyltransferase	RT	ns	0.299	0.729	0.017
	Phenylpropanoid biosynthesis					
TRINITY_DN6823_c0_g1_m.20755	Caffeic acid 3-O-methyltransferase	COMT1	1.249	0.049	2.209	0.014
TRINITY_DN10780_c0_g1_m.946	Omega-hydroxypalmitate O-feruloyl transferase	HHT1	ns	0.748	0.374	0.000248
TRINITY_DN8170_c0_g2_m.23343	Probable cinnamyl alcohol dehydrogenase	CAD6	ns	0.178	0.72	0.048
	Anthocyanin biosynthesis					
TRINITY_DN142_c0_g2_m.3870	Anthocyanidin 3-O-glucosyltransferase 2	FGT	ns	0.522	0.792	0.049
	Carotenoid biosynthesis					
TRINITY_DN2792_c0_g2_m.10610	Probable carotenoid cleavage dioxygenase 4	CCD4	ns	0.264956118	1.4016	0.038862
TRINITY_DN92199_c0_g1_m.25001	Lycopene beta cyclase	LCY1	ns	0.699025813	1.3876	0.014785649
	Antioxidation system					
TRINITY_DN4793_c1_g1_m.16452	Superoxide dismutase [Cu-Zn]	SODCP	1.3609	0.013743234	ns	0.204307412
TRINITY_DN13770_c0_g1_m.3537	Peroxidase 4	GSVIT00023967001	ns	0.866	3.076	0.043

Note: “ns” = no significant difference. Pitaya seedlings exposed to drought stress for 6 h and 3 days were designated as OS6H and OS3D, respectively, with the corresponding controls designated as NS6H and NS3D, respectively.

3.9. Validation of Proteomics Data by PRM

The label-free quantitative proteomics results were validated by PRM, which is a widely used and efficient method for precisely quantifying and verifying an array of target proteins of interest [31]. In this study, 21 DAPs annotated with GO terms and assigned to KEGG pathways were selected for the PRM analysis. Two unique peptides predicted to be stable were chosen for each protein, except for six DAPs, which had only one unique peptide. The relative protein abundance was expressed as the average of the two normalized peptide peak areas (Tables S4 and S5). The PRM results (Figure 5) were consistent with the label-free quantitative proteomics data.

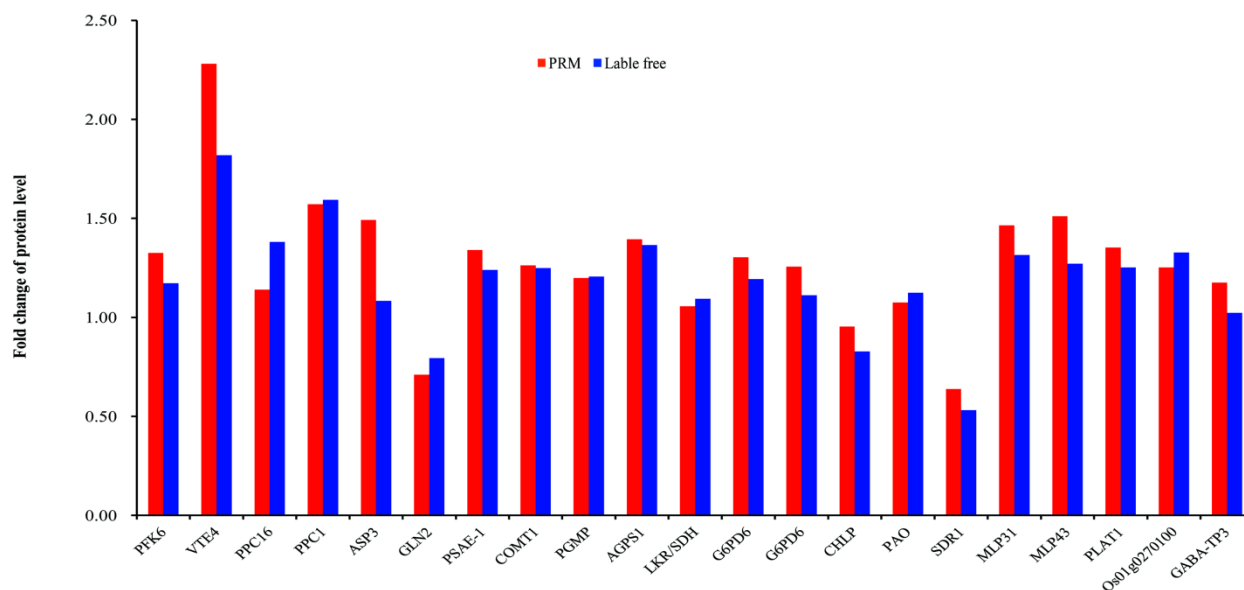


Figure 5. Validation of 21 selected DAPs via parallel reaction monitoring. The ordinate represents the OS6H/NS6H ratio. Abbreviated enzyme names are listed in Table S6.

4. Discussion

Drought is a major environmental factor affecting crop growth and yield. Treating plants with PEG is an effective method for simulating drought-stress conditions [32]. Pitaya is a widely cultivated crop in dry regions because of its relatively high tolerance to long-term drought stress and its ability to grow in low-quality soils [18]. Therefore, pitaya is a potentially useful research material for elucidating plant responses to drought stress [33]. In the current study, pitaya responses to drought stress induced by PEG were examined. The results provided evidence of the physiological and molecular changes at the protein level in pitaya exposed to drought stress.

4.1. Physiological Responses

To cope with drought stress, plants have evolved a range of physiological and biochemical mechanisms [34]. One of the most important mechanisms involves the accumulation of compatible osmolytes, including glycine betaine, soluble sugars, soluble proteins, and free proline [35]. In this study, pitaya plants were exposed to varying durations of drought stress. Compared with the control levels, the soluble protein and proline contents of stressed pitaya did not change significantly in the initial drought-treatment stage, but they increased significantly after three days of drought stress (Figure 1b,c). These results implied that osmoregulation is an important physiological mechanism enabling pitaya to adapt to drought conditions.

As the final product of lipid peroxidation, MDA is widely considered to be an important physiological marker of membrane system injuries induced by stresses [33]. Reactive oxygen species (ROS), such as H_2O_2 and O_2^- , are some of the most damaging molecules

in plants, capable of inducing changes at the cellular level, leading to membrane damage, protein oxidation, and alterations to DNA [36]. Earlier research concluded that MDA, H₂O₂, and O₂⁻ levels increased significantly following an exposure to drought stress [6]. The accumulation of ROS can be minimized by an array of nonenzymatic antioxidants (e.g., metabolites such as AsA, alpha-tocopherol, carotenoids, and GSH) and antioxidant enzymes (e.g., SOD and AsA-GSH cycle enzymes, including GR and APX) [37]. In accordance with the findings of Cao et al. [38], the physiological responses of pitaya to drought stress observed in this study included increased lipid peroxidation (as reflected by MDA, O₂⁻, and H₂O₂ levels) and enhanced antioxidant enzyme activities (e.g., SOD and APX) (Figure 1d–i). Moreover, tocopherol and carotenoid biosynthesis-related proteins were also identified as upregulated DAPs under drought-stress conditions (Table 5).

The ASA–GSH pathway, which maintains the ratios of reduced and oxidized AsA and GSH, affects the scavenging of ROS in plant cells [38]. These ratios are maintained by APX and GR [39]. An earlier investigation demonstrated that GR contents increased during exposure to drought stress [40]. In the present study, compared with the control levels, GR activities were significantly higher and lower in stressed pitaya samples at 6 and 18 h after initiating the drought-stress treatment, respectively (Figure 1g). These results indicated that GR is sensitive to drought stress and may be important for early pitaya responses to drought conditions.

4.2. Carbohydrate Metabolism

Carbon, which is indispensable for energy circulation and survival, is continuously metabolized in plants, even under adverse conditions [41]. Glycolysis is an important metabolic pathway for carbohydrate metabolism in all living organisms, and releases a small amount of energy in the absence of oxygen [42]. In the present study, most of the enzymes involved in glycolysis were upregulated DAPs in response to drought stress (Table 1). Among these enzymes, PFK6 is the rate-limiting enzyme for glycolysis and GAPC is widely considered to be responsive to drought stress [43]. Moreover, GAPC may restrict the accumulation of ROS and promote root growth in plants under drought conditions [42]. Interestingly, drought stress increased the ALDH3F1 content, but had the opposite effect on the accumulation of ALDH3H1. Accordingly, the aldehyde dehydrogenase family 3 members were differentially responsive to carbohydrate depletion, which was consistent with the findings of an earlier study [44] (Table 1). Stress-associated aldehyde dehydrogenases are important for scavenging ROS and catalyzing the oxidation of toxic aldehydes to produce nontoxic carboxylic acids. Additionally, they participate in several pathways and regulate diverse signal transductions [45]. Regarding starch and sucrose metabolism, starch degradation is promoted by the upregulated expression of some key genes, including those encoding ISA3 [46], DPEP [47], BAM9 [48], and AMY3 [49]. A previous study proved that the increases in soluble sugar contents in response to drought stress mainly resulted from the degradation and transformation of insoluble carbohydrates [50]. The activities of these enzymes may increase the soluble sugar content, which was consistent with the results of physiological determination (Table 1, Figure 1a). The drought-stress treatment in the current study had the opposite effects on the contents of two starch synthases (SS4 and SS1). A recent study indicated that SS4 contributed to the initiation of starch granules [48]. However, the exact roles of these enzymes in pitaya plants exposed to drought stress remain uncharacterized. Starch synthase activity affects chain elongation, as well as the branch placement resulting from the balanced activities of starch branching and debranching enzymes [51]. These results reflected the complexity of the changes in the expression of genes associated with the starch and sucrose metabolic pathway in pitaya plants under drought conditions.

4.3. Energy Metabolism

Several proteins associated with oxidative phosphorylation were activated in response to drought stress in pitaya plants (Table 2). Among these proteins, NADH dehydroge-

nase is involved in the classical electron-transport pathway coupled to ATP synthesis [52]. Additionally, V-ATPase uses energy from ATP hydrolysis to transport protons across membranes, which is important for various cellular processes, as well as acidification-independent processes (e.g., secretion and membrane fusion) [53]. The observed changes to NADH dehydrogenase and V-type proton ATPase subunits indicated that oxidative phosphorylation and ATP generation in pitaya were affected by drought. An earlier investigation proved that the excessive production of PUMP1, which inhibits ROS production under stress conditions by uncoupling the electrochemical gradient from ATP synthesis, induced a hypoxic response [54]. The increased accumulation of PUMP1 detected in this study implied that the relatively flexible energy metabolism of pitaya enables adaptations to drought stress [55]. The NADP-dependent malic enzyme and PPC contents increased in both comparisons. Their responses to drought stress were confirmed in a previous study [56] (Table 2). Moreover, NADP-dependent malic enzyme is considered to have multiple functions that enhance drought resistance. For example, it stabilizes the cytoplasmic pH, controls the stomatal aperture, and provides the essential reductive coenzyme NADPH during flavonoid and lignin biosynthesis. Furthermore, NADPH is crucial for ROS metabolism by the AsA–GSH pathway and NADPH-dependent thioredoxin reductase [57]. The abundance of LHCB7, which is the major antenna protein of photosystem II, increased in stressed pitaya at the 6 h time-point, but there was no difference between the control and stressed samples at 3 days after starting the stress treatment (Table 2). The changes to the accumulation of PSAE-1 and PSAH (i.e., two photosystem I reaction center subunits) were similar to those of LHCB7. The harvesting of light is the first step of photosynthesis. Consequently, the light-harvesting antenna must be regulated in response to the physiological status of plants and environmental signals [58]. A recent study indicated that PSAH expression is upregulated by high salinity and drought [59]. The observed increases in LHCB7, PSAE-1, and PSAH levels may reflect the temporary increase in the light-capturing ability and ion partitioning of pitaya plants under drought conditions. In contrast, the decrease in DEGP2 accumulation detected in this study may inhibit the primary cleavage of the photodamaged D1 protein in the central oxygen-evolving photosystem II reaction center, which has been reported for Arabidopsis plants exposed to salt and desiccation stresses [60]. Overall, drought stress enhances energy metabolism in pitaya, which may provide the energy necessary for initiating other metabolic pathways responsible for short-term adaptations to drought stress.

4.4. Amino Acid Metabolism

Amino acid metabolism plays an important role in signal transduction and osmoregulation [32]. Glutamine synthetase catalyzes the critical incorporation of inorganic ammonium into glutamine in an ATP-dependent manner [61]. A previous study confirmed that the abundance of glutamine synthetase increases in chickpea (*Cicer reticulatum* L.) grown under drought conditions [62]. However, another investigation indicated that the overexpression of genes that encode glutamine synthetase can increase the sensitivity of plants to drought stress [63]. Moreover, glutamine synthetase might influence stress-induced proline production [64]. The opposite changes to the accumulation of GLN2 and δ -OAT in the current study were indicative of a negative correlation between these enzymes (Table 3). In addition, the proline content changes lagged behind the changes to the abundance of δ -OAT (Figure 1c, Table 3), which is involved in proline synthesis, revealing an inconsistency between some physiological indices and changes in protein levels. Glutamate decarboxylase (GAD) is an enzyme that catalyzes the conversion of L-glutamate into γ -aminobutyric acid (GABA) [65], which accumulates in many plant species in response to environmental stresses [66]. The increased accumulation of GAD and GABA-TP3 in the current study suggested both enzymes may be critical for pitaya adaptations to drought stress. Furthermore, the contents of Asp3 increased substantially in pitaya subjected to drought stress, suggesting ASP3 may be important for the conversion and accumulation of amino acids that protect pitaya plants from the detrimental effects

of drought stress. Spermine and spermidine are useful osmotic solutes and important regulatory signals [67]. NOA1 and SPMS, detected as significantly downregulated DAPs only in the OS6H vs. NS6H comparison, may modulate the early drought stress responses of pitaya (Table 3). Additionally, ADT6, which catalyzes the final step in the biosynthesis of phenylalanine (i.e., the precursor for flavonoid biosynthesis) [68], was a downregulated DAP in the OS3D vs. NS3D comparison (Table 3). A similar change in protein abundance was observed for RT (Table 5). Taken together, drought stress significantly altered the balance between the conversion and accumulation of amino acids in pitaya.

4.5. GSH and AsA Metabolism

The ASA–GSH metabolism is an important antioxidative response pathway for plant responses to drought stress [38]. In the current study, the concentrations of only a few proteins related to this pathway decreased following the exposure to drought stress (Table 4). The increased abundance of most of the vital enzymes in this pathway (e.g., LGALDH, APX, GSTT1, and G6PD6) in the PEG-treated pitaya seedlings was consistent with the observed enhanced enzymatic activities (Figure 1g,i; Table 4). These results were in accordance with following the findings of other studies [69,70]. However, two UDP-glucose 6-dehydrogenases (UGD4 and UGD5) were revealed as downregulated DAPs in the OS6H vs. NS6H comparison, which was in contrast to the results of an earlier investigation [71]. In pitaya plants cultivated under drought conditions, these two enzymes may contribute to the formation of hemicellulose and pectin to strengthen cell walls [72]. Interestingly, the enhancer proteins identified as DAPs in this study (At5g05600) had rarely been reported as plant proteins responsive to drought stress. Hence, they are potentially interesting candidate proteins for future studies on drought-resistant germplasm.

4.6. Secondary Metabolism

Ten DAPs were classified as proteins affecting secondary metabolism (Table 5). Three proteins associated with lignin monomer synthesis accumulated differentially between the control and stressed plants. More specifically, COMT1 was an upregulated DAP in the two comparisons, whereas CAD6 and HHT1 were detected as downregulated DAPs in the OS3D vs. NS3D comparison. The downregulation of CAD6 and HHT1 may have been because lignin accumulation is restricted in pitaya under drought-stress conditions [73,74]. The accumulation of COMT1 generally decreases in response to drought stress. The observed increase in COMT1 abundance in this study is suggestive of additional roles for this protein in the melatonin biosynthesis pathway [75]. Although RT has been identified in *Petunia hybrida* (J. D. Hooker) Vilmorin [76], the effects of drought stress on this protein have not been elucidated. Apocarotenoid compounds, including hormones, pigments, and volatiles, have diverse communication-related functions in plants. Apocarotenoids are produced via the cleavage of carotenoids by carotenoid cleavage dioxygenase (CCD). An earlier study revealed CsCCD4c expression is upregulated by wounding, heat, and drought stress [77]. In tobacco, LCY1 is likely a cyclization-catalyzing enzyme involved in carotenoid accumulation, but it also mediates drought-stress tolerance [78]. The identification of CCD4 and LCY1 as upregulated DAPs in the OS3D vs. NS3D comparison provided additional evidence that these types of enzymes protect plants from drought stress. Additionally, VET4 is reportedly a potential biomarker of oxidative damage [79]. The drought-induced increase in the abundance of VET4 observed in the current study may be involved in mitigating damages due to ROS and lipid peroxidation.

5. Conclusions

In summary, in pitaya, drought stress increased osmolyte accumulation, lipid peroxidation, and antioxidant enzyme activities. Proteomic data revealed several pathways were activated in pitaya plants, including carbohydrate and energy metabolism at 6 h and 3 days after starting a simulated drought treatment. Other metabolic activities, including pathways related to aspartate, glutamate, GSH, and secondary metabolites, were affected

more after 3 days than after 6 h. In contrast, photosynthesis and arginine metabolism were modulated solely at the 6 h time-point. Moreover, some key proteins identified in this study, including mitochondrial uncoupling protein 1 (PUMP1), 2-oxoglutarate-dependent dioxygenase (At5g05600), anthocyanidin-3-O-glucoside rhamnosyltransferase (RT), and omega-hydroxypalmitate O-feruloyl transferase (HHT1), have rarely been reported as responsive to drought stress. The possible functions of these proteins influencing drought resistance will need to be experimentally verified. A model for the comparative physiological and proteomic analysis of pitaya responses to PEG-induced drought stress is presented in Figure 6. The high drought tolerance of pitaya was attributed to its high osmotic adjustment capacity and great ability to orchestrate its enzymatic and nonenzymatic antioxidant systems, thus avoiding significant oxidative damage.

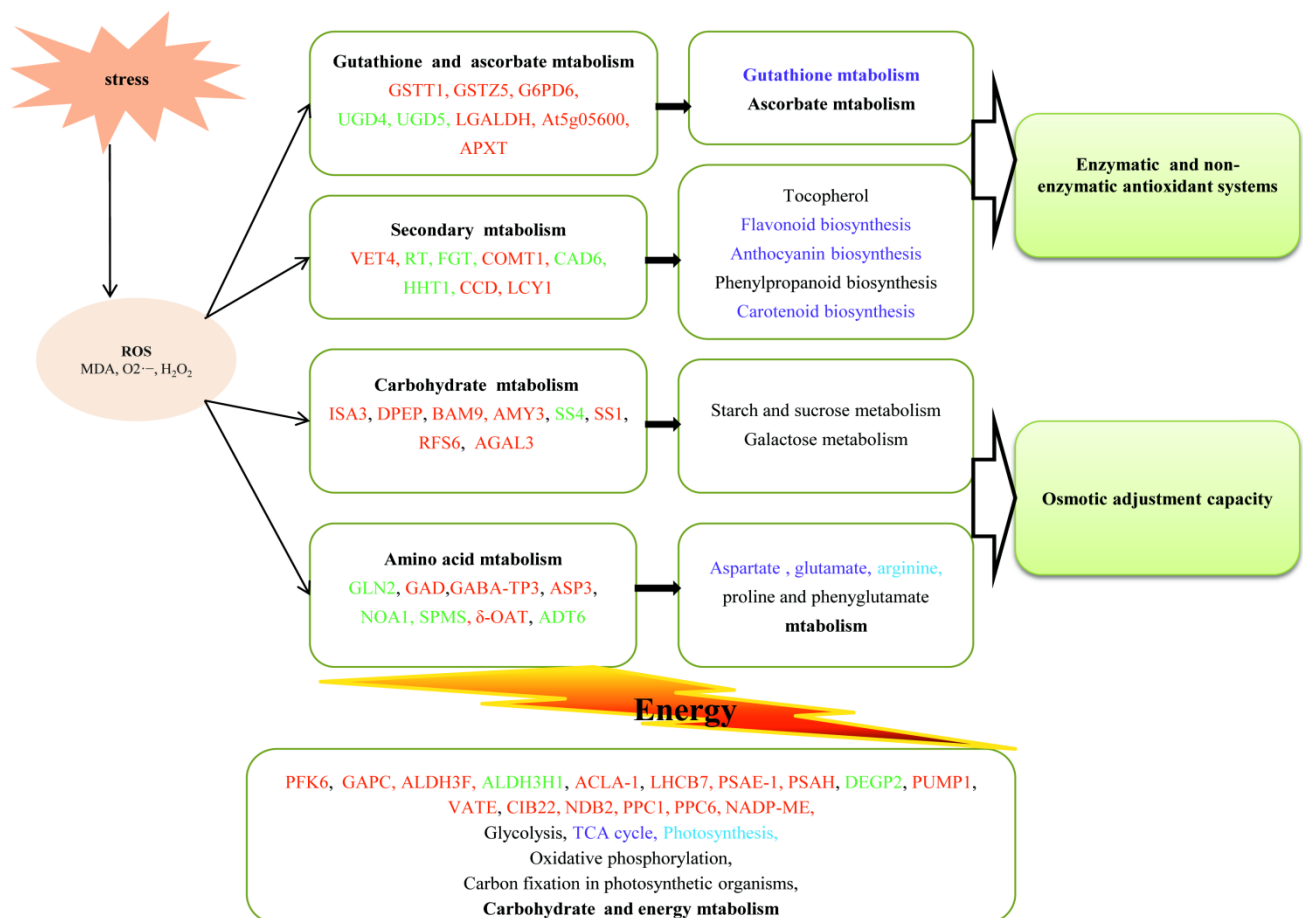


Figure 6. Model of pitaya responses to PEG-induced drought stress developed according to physiological and proteomic changes. Abbreviated enzyme names are listed in Table S6. Enzymes in green and red represent downregulated and upregulated proteins, respectively. Metabolic pathways in light blue and purple were mainly affected at 6 h and 3 days after initiating a drought-stress treatment, respectively.

Supplementary Materials: The following are available online at <https://www.mdpi.com/article/10.3390/agriculture11070632/s1>, Figure S1: The drought experiment design for pitaya. Pitaya seedlings exposed to drought stress for 6 h and 3 days were designated as OS6H and OS3D, respectively, with the corresponding controls designated as NS6H and NS3D, respectively; Figure S2: Distribution of the number of peptides per protein; Table S1: Detailed information for all identified proteins; Table S2: DAPs in pitaya at 6 h after starting the drought-stress treatment; Table S3: DAPs in pitaya at 3 days after starting the drought-stress treatment; Table S4: Peptide results for 21 DAPs selected for the PRM analysis of pitaya plants exposed to PEG-induced drought stress for 6 h; Table S5: Protein results for 21 DAPs selected for the PRM analysis of pitaya plants exposed to PEG-induced drought stress for 6 h; Table S6: Abbreviated enzyme names in the model.

Author Contributions: X.W. conceived and designed the research; A.W. performed most of the experiments, analyzed the data, and prepared the manuscript; C.M. and Z.Q. contributed analysis tools and offered technical support; A.W. carried out the experiments with the help of H.M. All authors have read and approved the final version of the manuscript.

Funding: This project was supported by grants from the National Natural Science Foundation of China (31760566, 32060663), Science and Technology Support Plan in Guizhou, China (2018-2282, 2020-1Y018), and the Innovation Talent Program of Guizhou Province, China (2016-4010).

Institutional Review Board Statement: Not applicable.

Informed Consent Statement: Not applicable.

Data Availability Statement: The datasets supporting the conclusions of this article are included within the article and its additional files. The datasets used and/or analyzed during the current study are available from the authors on reasonable request (Aihua Wang, 118wah@163.com; Guang Qiao, 13518504594@163.com).

Acknowledgments: Not applicable.

Conflicts of Interest: The authors declare no conflict of interest.

Abbreviations

PEG	Polyethylene glycol
MDA	Malondialdehyde
O ₂ ⁻	Superoxide anion
H ₂ O ₂	Hydrogen peroxide
SOD	Superoxide dismutase
ASA	Ascorbate
GSH	Glutathione
APX	Ascorbic peroxidase
ROS	Reactive oxygen species
GO	Gene ontology
DAPs	Differentially accumulated proteins
PUMP1	Mitochondrial uncoupling protein 1
LHCB7	Chlorophyll a-b binding protein 7
PSAE-1	Photosystem I reaction center subunit IV
PSAH	Photosystem I reaction center subunit VI
GAPC	Glyceraldehyde-3-phosphate dehydrogenase
SS	Starch synthase
KEGG	Kyoto Encyclopedia of Genes and Genomes
GAD	Glutamate decarboxylase
ASP3	Aspartate aminotransferase 3
OAT	Ornithine aminotransferase
NOA1	NO-associated protein 1
SPMS	Spermine synthase
PRM	Parallel reaction monitoring
G6PD6	Glucose-6-phosphate 1-dehydrogenase 6
At5g05600	Probable 2-oxoglutarate-dependent dioxygenase
GST	Glutathione S-transferase
LGALDH	L-galactose dehydrogenase
VET4	Probable tocopherol O-methyltransferase
CCD	Probable carotenoid cleavage dioxygenase
RT	Anthocyanidin-3-O-glucoside rhamnosyltransferase
COMT1	Caffeic acid 3-O-methyltransferase
HHT1	Omega-hydroxypalmitate O-feruloyl transferase

References

1. Suleymanov, S.Y.; Aliyeva, D.R.; Mammadov, A.C.; Aliyev, J.A. Drought-induced changes in photosynthetic apparatus and antioxidant components of wheat (*Triticum durum* Desf.) varieties. *Photosynth. Res.* **2016**, *130*, 215–223.
2. Anwar, A.; She, M.; Wang, K.; Riaz, B.; Ye, X. Biological roles of ornithine aminotransferase (OAT) in plant stress tolerance: Present progress and future perspectives. *Int. J. Mol. Sci.* **2018**, *19*, 3681. [[CrossRef](#)]
3. Thirunavukkarasu, N.; Sharma, R.; Singh, N.; Shiriga, K.; Mohan, S.; Mittal, S.; Mittal, S.; Mallikarjuna, M.G.; Rao, A.R.; Dash, P.K.; et al. Genomewide expression and functional interactions of genes under drought stress in maize. *Int. J. Genom.* **2017**, 1–14. [[CrossRef](#)]
4. Claeys, H.; Inzé, D. The agony of choice: How plants balance growth and survival under water-limiting conditions. *Plant Physiol.* **2013**, *162*, 1768–1779. [[CrossRef](#)] [[PubMed](#)]
5. Zhao, P.; Liu, P.; Shao, J.; Li, C.; Wang, B.; Guo, X.; Yan, B.; Xia, Y.; Peng, M. Analysis of different strategies adapted by two cassava cultivars in response to drought stress: Ensuring survival or continuing growth. *J. Exp. Bot.* **2015**, *66*, 1477–1488. [[CrossRef](#)] [[PubMed](#)]
6. Zhang, C.; Shi, S. Physiological and proteomic responses of contrasting Alfalfa (*Medicago sativa* L.) varieties to PEG-Induced osmotic stress. *Front. Plant Sci.* **2018**, *9*, 242. [[CrossRef](#)] [[PubMed](#)]
7. Sharma, M.; Gupta, S.K.; Majumder, B.; Maurya, V.K.; Deeba, F.; Alam, A.; Pandey, V. Salicylic acid mediated growth, physiological and proteomic responses in two wheat varieties under drought stress. *J. Proteom.* **2017**, *163*, 28–51. [[CrossRef](#)]
8. Ma, X.; Wang, P.; Zhou, S.; Sun, Y.; Liu, N.; Li, X.; Hou, Y. De novo transcriptome sequencing and comprehensive analysis of the drought-responsive genes in the desert plant *Cynanchum komarovii*. *BMC Genom.* **2015**, *16*, 753. [[CrossRef](#)]
9. Carmo, L.S.T.; Martins, A.C.Q.; Martins, C.C.C.; Passos, M.A.S.; Silva, L.P.; Araujo, A.C.G.; Brasileiro, A.C.M.; Miller, R.N.G.; Guimarães, P.M.; Mehta, A. Comparative proteomics and gene expression analysis in *Arachis duranensis* reveal stress response proteins associated to drought tolerance. *J. Proteom.* **2019**, *192*, 299–310. [[CrossRef](#)]
10. Gharechahi, J.; Hajirezaei, M.R.; Salekdeh, G.H. Comparative proteomic analysis of tobacco expressing cyanobacterial flavodoxin and its wild type under drought stress. *J. Plant Physiol.* **2015**, *175*, 48–58. [[CrossRef](#)]
11. Wang, X.; Oh, M.; Sakata, K.; Komatsu, S. Gel-free/label-free proteomic analysis of root tip of soybean over time under flooding and drought stresses. *J. Proteom.* **2016**, *13*, 42–55. [[CrossRef](#)]
12. Lalit, A.; Swati, G.; Mishra, S.K.; Garima, P.; Susheel, K.; Chauhan, P.S.; Chakrabarty, D.; Nautiyal, C.S. Elucidation of complex nature of PEG induced drought-stress response in rice root using comparative proteomics approach. *Front. Plant Sci.* **2016**, *7*, 1466.
13. Li, N.; Zhang, S.; Liang, Y.; Qi, Y.; Chen, J.; Zhu, W.; Zhang, L. Label-free quantitative proteomic analysis of drought stress-responsive late embryogenesis abundant proteins in the seedling leaves of two wheat (*Triticum aestivum* L.) genotypes. *J. Proteom.* **2018**, *172*, 122–142. [[CrossRef](#)]
14. Dong, H.; Li, Y.; Fan, H.; Zhou, D.; Li, H. Quantitative proteomics analysis reveals resistance differences of banana cultivar ‘Brazilian’ to *Fusarium oxysporum* f. sp. *cubense* races 1 and 4. *J. Proteom.* **2019**, *203*, 103376. [[CrossRef](#)] [[PubMed](#)]
15. Moosavi, S.S.; Abdi, F.; Abdollahi, M.R.; Tahmasebi-Enferadi, S.; Maleki, M. Phenological, morpho-physiological and proteomic responses of *Triticum boeoticum* to drought stress. *Plant Physiol. Biochem.* **2020**, *156*, 95–104. [[CrossRef](#)] [[PubMed](#)]
16. Chen, Z.; Xu, J.; Wang, F.; Wang, L.; Xu, Z. Morpho-physiological and proteomic responses to water stress in two contrasting tobacco varieties. *Sci. Rep.* **2019**, *9*, 18523. [[CrossRef](#)] [[PubMed](#)]
17. Ortiz, T.A.; Takahashi, L.S. Physical and chemical characteristics of pitaya fruits at physiological maturity. *Genet. Mol. Res.* **2015**, *14*, 14422–14439. [[CrossRef](#)] [[PubMed](#)]
18. Hua, Q.; Chen, C.; Tel Zur, N.; Wang, H.; Wu, J.; Chen, J.; Zhang, Z.; Zhao, J.; Hu, G.; Qin, Y. Metabolomic characterization of pitaya fruit from three red-skinned cultivars with different pulp colors. *Plant Physiol. Biochem.* **2018**, *126*, 117–125. [[CrossRef](#)] [[PubMed](#)]
19. Nie, Q.; Qiao, G.; Peng, L.; Wen, X. Transcriptional activation of long terminal repeat retrotransposon sequences in the genome of pitaya under abiotic stress. *Plant Physiol. Biochem.* **2019**, *135*, 460–468. [[CrossRef](#)] [[PubMed](#)]
20. Fan, Q.J.; Yan, F.X.; Qiao, G.; Zhang, B.X.; Wen, X.P. Identification of differentially-expressed genes potentially implicated in drought response in pitaya (*Hylocereus undatus*) by suppression subtractive hybridization and cDNA microarray analysis. *Gene* **2014**, *533*, 322–331. [[CrossRef](#)] [[PubMed](#)]
21. Hoagland, D.; Arnon, D.I. The water culture method for growing plants without soil. *Calif. Agric. Exp. Stn. Circ.* **1950**, *347*, 32.
22. Buysse, J.; Merckx, R. An improved colorimetric method to quantify sugar content of plant tissue. *J. Exp. Bot.* **1993**, *44*, 1627–1629. [[CrossRef](#)]
23. Bradford, M.M. A rapid and sensitive method for the quantitation of microgram quantities of protein utilizing the principle of protein-dye binding. *Anal. Biochem.* **1976**, *72*, 248–254. [[CrossRef](#)]
24. Bates, L.S.; Waldren, R.P.; Teare, I.D. Rapid determination of free proline for water-stress studies. *Plant Soil.* **1973**, *39*, 205–207. [[CrossRef](#)]
25. Castrejón, S.E.; Yatsimirsky, A.K. Cyclodextrin enhanced fluorimetric determination of malonaldehyde by the thiobarbituric acid method. *Talanta* **1997**, *44*, 951–957. [[CrossRef](#)]
26. Lin, Y.F.; Lin, Y.X.; Lin, H.T.; Zhang, S.; Chen, Y.H.; Shi, J. Inhibitory effects of propyl gallate on browning and its relationship to active oxygen metabolism in pericarp of harvested longan fruit. *LWT Food Sci. Technol.* **2015**, *60*, 1122–1128. [[CrossRef](#)]

27. Sim, Y.H.; Yao, J.M.; Hou, Y.S.; Wang, L.; Zhao, L.C. Variations of hydrogen peroxide and catalase expression in *Bombyx* eggs during diapause initiation and termination. *Arch. Insect Biochem. Physiol.* **2011**, *77*, 72–80. [[CrossRef](#)] [[PubMed](#)]
28. García-Triana, A.; Zenteno-Savín, T.; Peregrino-Urriarte, A.B.; Yepiz-Plascencia, G. Hypoxia, reoxygenation and cytosolic manganese superoxide dismutase (cMnSOD) silencing in *Litopenaeus vannamei*: Effects on cMnSOD transcripts, superoxide dismutase activity and superoxide anion production capacity. *Dev. Comp. Immunol.* **2010**, *34*, 1230–1235. [[CrossRef](#)]
29. Foster, J.G.; Hess, J.L. Responses of superoxide dismutase and glutathione reductase activities in cotton leaf tissue exposed to an atmosphere enriched in oxygen. *Plant Physiol.* **1980**, *66*, 482–487. [[CrossRef](#)]
30. Ullah, S.; Kolo, Z.; Egbichi, I.; Keyster, M.; Ludidi, N. Nitric oxide influences glycine betaine content and ascorbate peroxidase activity in maize. *S. Afr. J. Bot.* **2016**, *105*, 218–225. [[CrossRef](#)]
31. Zhao, Y.L.; Huang, X.; Liu, L.W.; Wang, P.Y.; Long, Q.S.; Tao, Q.Q.; Li, Z.; Yang, S. Identification of racemic and chiral carbazole derivatives containing an isopropanolamine linker as prospective surrogates against plant pathogenic bacteria: In vitro and in vivo assays and quantitative proteomics. *J. Agric. Food Chem.* **2019**, *67*, 7512–7525. [[CrossRef](#)]
32. Cui, G.; Zhao, Y.; Zhang, J.; Chao, M.; Xie, K.; Zhang, C.; Sun, F.; Liu, S.; Xi, Y. Proteomic analysis of the similarities and differences of soil drought and polyethylene glycol stress responses in wheat (*Triticum aestivum* L.). *Plant Mol. Biol.* **2019**, *100*, 391–410. [[CrossRef](#)]
33. Wang, A.H.; Yang, L.; Yao, X.Z.; Wen, X.P. Overexpression of the pitaya phosphoethanolamine N -methyltransferase gene (*HpPEAMT*) enhanced simulated drought stress in tobacco. *Plant Cell Tissue Organ Cult.* **2021**, *146*, 29–40. [[CrossRef](#)]
34. You, J.; Hu, H.; Xiong, L. An ornithine δ -aminotransferase gene *OsOAT* confers drought and oxidative stress tolerance in rice. *Plant Sci.* **2012**, *197*, 59–69. [[CrossRef](#)] [[PubMed](#)]
35. Adamipour, N.; Khosh-Khui, M.; Salehi, H.; Razi, H.; Karami, A.; Moghadam, A. Metabolic and genes expression analyses involved in proline metabolism of two rose species under drought stress. *Plant Physiol. Biochem.* **2020**, *155*, 105–113. [[CrossRef](#)] [[PubMed](#)]
36. Faize, M.; Burgos, L.; Faize, L.; Piqueras, A.; Nicolas, E.; Barba-Espin, G.; Clemente-Moreno, M.J.; Alcobendas, R.; Artlip, T.; Hernandez, J.A. Involvement of cytosolic ascorbate peroxidase and Cu/Zn-superoxide dismutase for improved tolerance against drought stress. *J. Exp. Bot.* **2011**, *62*, 2599–2613. [[CrossRef](#)] [[PubMed](#)]
37. Ansari, W.A.; Atri, N.; Ahmad, J.; Qureshi, M.I.; Singh, B.; Kumar, R.; Rai, V.; Pandey, S. Drought mediated physiological and molecular changes in muskmelon (*Cucumis melo* L.). *PLoS ONE* **2019**, *14*, e0222647. [[CrossRef](#)]
38. Cao, Y.; Luo, Q.; Tian, Y.; Meng, F. Physiological and proteomic analyses of the drought stress response in *Amygdalus Mira* (Koehne) Yü et Lu roots. *BMC Plant Biol.* **2017**, *17*, 53. [[CrossRef](#)]
39. Asada, K. The water-water cycle in chloroplasts: Scavenging of active oxygens and dissipation of excess photons. *Annu. Rev. Plant Physiol. Plant Mol. Biol.* **1999**, *50*, 601–639. [[CrossRef](#)]
40. Iqbal, N.; Hussain, S.; Raza, M.A.; Yang, C.Q.; Safdar, M.E.; Brestic, M.; Aziz, A.; Hayyat, M.S.; Asghar, M.A.; Wang, X.C.; et al. Drought tolerance of soybean (*Glycine max* L. Merr.) by improved photosynthetic characteristics and an efficient antioxidant enzyme activities under a split-root system. *Front. Physiol.* **2019**, *10*, 786. [[CrossRef](#)]
41. Hao, P.; Zhu, J.; Gu, A.; Lv, D.; Ge, P.; Chen, G.; Li, X.; Yan, Y. An integrative proteome analysis of different seedling organs in tolerant and sensitive wheat cultivars under drought stress and recovery. *Proteomics* **2015**, *15*, 1544–1563. [[CrossRef](#)] [[PubMed](#)]
42. Zhang, L.; Zhang, H.; Yang, S. Cytosolic TaGAPC2 enhances tolerance to drought stress in transgenic arabidopsis plants. *Int. J. Mol. Sci.* **2020**, *21*, 7499. [[CrossRef](#)] [[PubMed](#)]
43. Zhang, L.; Xu, Z.; Ji, H.; Zhou, Y.; Yang, S. *TaWRKY40* transcription factor positively regulate the expression of *TaGAPC1* to enhance drought tolerance. *BMC Genom.* **2019**, *20*, 795. [[CrossRef](#)]
44. Huang, W.; Ma, X.; Wang, Q.; Gao, Y.; Xue, Y.; Niu, X.; Yu, G.; Liu, Y. Significant improvement of stress tolerance in tobacco plants by overexpressing a stress-responsive aldehyde dehydrogenase gene from maize (*Zea mays*). *Plant Mol. Biol.* **2008**, *68*, 451–463. [[CrossRef](#)] [[PubMed](#)]
45. Kirch, H.H.; Schlingensiepen, S.; Kotchoni, S.; Sunkar, R.; Bartels, D. Detailed expression analysis of selected genes of the aldehyde dehydrogenase (*ALDH*) gene superfamily in *Arabidopsis thaliana*. *Plant Mol. Biol.* **2005**, *57*, 315–332. [[CrossRef](#)] [[PubMed](#)]
46. Ferreira, S.J.; Senning, M.; Fischer-Stettler, M.; Streb, S.; Ast, M.; Neuhaus, H.E.; Zeeman, S.C.; Sonnewald, S.; Sonnewald, U. Simultaneous silencing of isoamylases ISA1, ISA2 and ISA3 by multi-target RNAi in potato tubers leads to decreased starch content and an early sprouting phenotype. *PLoS ONE* **2017**, *12*, e0181444. [[CrossRef](#)]
47. Steichen, J.M.; Petty, R.V.; Sharke, T.D. Domain characterization of a 4- α -glucanotransferase essential for maltose metabolism in photosynthetic leaves. *J. Biol. Chem.* **2008**, *283*, 20797–20804. [[CrossRef](#)]
48. Malinova, I.; Alseekh, S.; Feil, R.; Fernie, A.R.; Baumann, O.; Schöttler, M.A.; Lunn, J.E.; Fettke, J. Starch synthase 4 and plastidial phosphorylase differentially affect starch granule number and morphology. *Plant Physiol.* **2017**, *174*, 73–85. [[CrossRef](#)]
49. Li, C.Y.; Weiss, D.; Goldschmidt, E.E. Effects of carbohydrate starvation on gene expression in citrus root. *Planta* **2003**, *217*, 11–20. [[CrossRef](#)]
50. Griffiths, H.; Parry, M.A.J. Plant responses to water stress. *Ann. Bot.* **2002**, *89*, 801–802. [[CrossRef](#)]
51. Szydlowski, N.; Ragel, P.; Hennen-Bierwagen, T.A.; Planchot, V.; Myers, A.M.; Mérida, A.; d’Hulst, C.; Wattedled, F. Integrated functions among multiple starch synthases determine both amylopectin chain length and branch linkage location in arabidopsis leaf starch. *J. Exp. Bot.* **2011**, *62*, 4547–4559. [[CrossRef](#)]

52. Sweetman, C.S.; Waterman, C.D.; Rainbird, B.M.; Smith, P.M.C.; Jenkins, C.D.; Day, D.A.; Soole, K.L. AtNDB2 is the main external NADH dehydrogenase in mitochondria and is important for tolerance to environmental stress. *Plant Physiol.* **2019**, *181*, 774–788. [[CrossRef](#)]
53. Sun-Wada, G.H.; Wada, Y. Role of vacuolar-type proton ATPase in signal transduction. *Biochim. Biophys. Acta* **2015**, *1847*, 1166–1172. [[CrossRef](#)]
54. Barreto, P.; Okura, V.K.; Neshich, I.A.; Maia Ide, G.; Arruda, P. Overexpression of UCP1 in tobacco induces mitochondrial biogenesis and amplifies a broad stress response. *BMC Plant Biol.* **2014**, *14*, 144. [[CrossRef](#)]
55. Barreto, P.; Okura, V.; Pena, I.A.; Maia, R.; Maia, I.G.; Arruda, P. Overexpression of mitochondrial uncoupling protein 1 (UCP1) induces a hypoxic response in *Nicotiana tabacum* leaves. *J. Exp. Bot.* **2016**, *67*, 301–313. [[CrossRef](#)]
56. Wen, Z.; Zhang, M. Possible involvement of phosphoenolpyruvate carboxylase and NAD-malic enzyme in response to drought stress. A case study: A succulent nature of the C₄-NAD-ME type desert plant, *Salsola lanata* (Chenopodiaceae). *Funct. Plant Biol.* **2017**, *44*, 1219–1228. [[CrossRef](#)]
57. Chen, Q.; Wang, B.; Ding, H.; Zhang, J.; Li, S. Review: The role of NADP-malic enzyme in plants under stress. *Plant Sci.* **2019**, *281*, 206–212. [[CrossRef](#)] [[PubMed](#)]
58. Silva, J.; Kim, Y.J.; Sukweenadhi, J.; Rahimi, S.; Kwon, W.S.; Yang, D.C. Molecular characterization of 5 chlorophyll *a/b*-binding protein genes from panax ginseng meyer and their expression analysis during abiotic stresses. *Photosynthetica* **2016**, *54*, 446–458. [[CrossRef](#)]
59. Hao, X.; Li, J.; Gao, S.; Tuerxun, Z.; Chang, X.; Hu, W.; Chen, G.; Huang, Q. *SsPsaH*, a H subunit of the photosystem I reaction center of *Suaeda salsa*, confers the capacity of osmotic adjustment in tobacco. *Genes Genom.* **2020**, *42*, 1455–1465. [[CrossRef](#)] [[PubMed](#)]
60. Hausstühl, K.; Andersson, B.; Adamska, I. A chloroplast DegP2 protease performs the primary cleavage of the photodamaged D1 protein in plant photosystem II. *EMBO J.* **2011**, *20*, 713–722.
61. James, D.; Borphukan, B.; Fartyal, D.; Ram, B.; Singh, J.; Manna, M.; Sheri, V.; Panditi, V.; Yadav, R.; Achary, V.M.M.; et al. Concurrent overexpression of *OsGS1;1* and *OsGS2* genes in transgenic Rice (*Oryza sativa* L.): Impact on tolerance to abiotic stresses. *Front. Plant Sci.* **2018**, *21*, 786. [[CrossRef](#)]
62. Cevik, S.; Akpınar, G.; Yildizli, A.; Kasap, M.; Karaosmanoglu, K.; Unyayar, S. Comparative physiological and leaf proteome analysis between drought-tolerant chickpea *Cicer reticulatum* and drought-sensitive chickpea *C. arietinum*. *J. Biosci.* **2019**, *44*, 20. [[CrossRef](#)]
63. Cai, H.; Zhou, Y.; Xiao, J.; Li, X.; Zhang, Q.; Lian, X. Overexpressed glutamine synthetase gene modifies nitrogen metabolism and abiotic stress responses in rice. *Plant Cell Rep.* **2009**, *28*, 527–537. [[CrossRef](#)]
64. Díaz, P.; Betti, M.; Sánchez, D.H.; Udvardi, M.K.; Monza, J.; Márquez, A.J. Deficiency in plastidic glutamine synthetase alters proline metabolism and transcriptomic response in *Lotus japonicus* under drought stress. *New Phytol.* **2010**, *188*, 1001–1013. [[CrossRef](#)]
65. Hyun, T.K.; Eom, S.H.; Han, X.; Kim, J.S. Evolution and expression analysis of the soybean glutamate decarboxylase gene family. *J. Biosci.* **2014**, *39*, 899–907. [[CrossRef](#)] [[PubMed](#)]
66. Bao, H.; Chen, X.; Lv, S.; Jiang, P.; Feng, J.; Fan, P.; Nie, L.; Li, Y. Virus-induced gene silencing reveals control of reactive oxygen species accumulation and salt tolerance in tomato by γ -aminobutyric acid metabolic pathway. *Plant Cell Environ.* **2015**, *38*, 600–613. [[CrossRef](#)] [[PubMed](#)]
67. Li, Z.; Zhang, Y.; Xu, Y.; Zhang, X.; Peng, Y.; Ma, X.; Huang, L.; Yan, Y. The physiological and iTRAQ-based proteomic analyses reveal the function of spermidine on improving drought tolerance in white clover. *J. Proteome Res.* **2016**, *15*, 1563–1579. [[CrossRef](#)] [[PubMed](#)]
68. Wang, X.C.; Wu, J.; Guan, M.L.; Zhao, C.H.; Geng, P.; Zhao, Q. *Arabidopsis* MYB4 plays dual roles in flavonoid biosynthesis. *Plant J.* **2020**, *101*, 637–652. [[CrossRef](#)] [[PubMed](#)]
69. Ma, L.; Zhang, Y.; Meng, Q.; Shi, F.; Liu, J.; Li, Y. Molecular cloning, identification of GSTs family in sunflower and their regulatory roles in biotic and abiotic stress. *World J. Microbiol. Biotechnol.* **2018**, *34*, 109. [[CrossRef](#)]
70. Wang, X.; Ruan, M.; Wan, Q.; He, W.; Yang, L.; Liu, X.; He, L.; Yan, L.; Bi, Y. Nitric oxide and hydrogen peroxide increase glucose-6-phosphate dehydrogenase activities and expression upon drought stress in soybean roots. *Plant Cell Rep.* **2020**, *39*, 63–73. [[CrossRef](#)]
71. Vítámvás, P.; Urban, M.O.; Škodáček, Z.; Kosová, K.; Pitelková, I.; Vítámvás, J.; Renaut, J.; Prášil, I.T. Quantitative analysis of proteome extracted from barley crowns grown under different drought conditions. *Front. Plant Sci.* **2015**, *6*, 479. [[CrossRef](#)] [[PubMed](#)]
72. Johansson, H.; Sterky, F.; Amini, B.; Lundeberg, J.; Kleczkowski, L.A. Molecular cloning and characterization of a cDNA encoding poplar UDP-glucose dehydrogenase, a key gene of hemicellulose/pectin formation. *Biochim. Biophys. Acta* **2021**, *1576*, 53–58. [[CrossRef](#)]
73. Gupta, S.; Mishra, S.K.; Misra, S.; Pandey, V.; Agrawal, L.; Nautiyal, C.S.; Chauhan, P.S. Revealing the complexity of protein abundance in chickpea root under drought-stress using a comparative proteomics approach. *Plant Physiol. Biochem.* **2020**, *151*, 88–102. [[CrossRef](#)] [[PubMed](#)]
74. Shi, C.H.; Qi, B.X.; Wang, X.Q.; Shen, L.Y.; Luo, J.; Zhang, Y.X. Proteomic analysis of the key mechanism of exocarp russet pigmentation of semi-russet pear under rainwater condition. *Sci. Hortic.* **2019**, *254*, 178–186. [[CrossRef](#)]

75. Li, W.; Lu, J.; Lu, K.; Yuan, J.; Huang, J.; Du, H.; Li, J. Cloning and phylogenetic analysis of *brassica napus* L. *Caffeic acid O-Methyltransferase 1* gene family and its expression pattern under drought stress. *PLoS ONE* **2016**, *11*, e0165975. [[CrossRef](#)]
76. Mato, M.; Ozeki, Y.; Itoh, Y.; Higeta, D.; Yoshitama, K.; Teramoto, S.; Aida, R.; Ishikura, N.; Shibata, M. Isolation and characterization of a cDNA clone of UDP-galactose: Flavonoid 3-O-galactosyltransferase (UF3GaT) expressed in *Vigna mungo* seedlings. *Plant Cell Physiol.* **1998**, *39*, 1145–1155. [[CrossRef](#)] [[PubMed](#)]
77. Rubio-Moraga, A.; Rambla, J.L.; Fernández-de-Carmen, A.; Trapero-Mozos, A.; Ahrazem, O.; Orzáez, D.; Granell, A.; Gómez-Gómez, L. New target carotenoids for CCD4 enzymes are revealed with the characterization of a novel stress-induced carotenoid cleavage dioxygenase gene from *Crocus sativus*. *Plant Mol. Biol.* **2014**, *86*, 555–569. [[CrossRef](#)] [[PubMed](#)]
78. Shi, Y.; Guo, J.; Zhang, W.; Jin, L.; Liu, P.; Chen, X.; Li, F.; Wei, P.; Li, Z.; Li, W.; et al. Cloning of the *Lycopene β -cyclase* Gene in *Nicotiana tabacum* and its overexpression confers salt and drought tolerance. *Int. J. Mol. Sci.* **2015**, *16*, 30438–30457. [[CrossRef](#)]
79. Yang, M.; Fan, Z.; Xie, Y.; Fang, L.; Wang, X.; Yuan, Y.; Li, R. Transcriptome analysis of the effect of bisphenol A exposure on the growth, photosynthetic activity and risk of microcystin-LR release by *Microcystis aeruginosa*. *J. Hazard. Mater.* **2020**, *397*, 122746. [[CrossRef](#)]